AD A030931

AFOSR - TR - 76 - 1100

LOCKHEED

MISSILES & SPACE COMPANY INC • SUNNYVALE CALIFORNIA

A SUBSIDIARY OF LOCKHEED AIRCRAFT CORPORATION

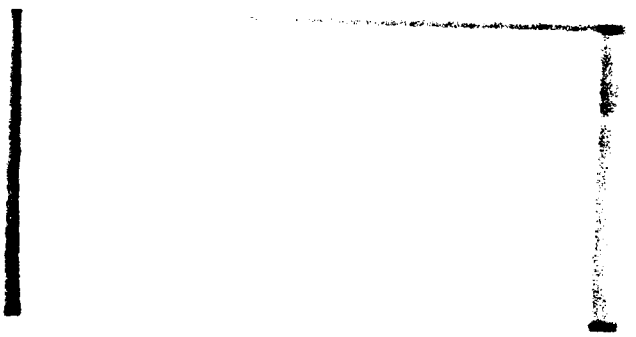

AIR FORCE OFFICE OF SCIENTIFIC RESEARCH ([redacted])
NOTICE OF TRANSMITTAL TO DDC
This technical report has been reviewed and is
approved for public release IAW AFR 190-12 (7b).
Distribution is unlimited.
A. D. BLOSE
Technical Information Officer

(11)

LMSC D508187

Final Report

CORKSCREW EFFECT STUDY

M. W. Munn
R. S. Benson

August 1976

Submitted to
AIR FORCE OFFICE OF SCIENTIFIC RESEARCH (AFSC)
Under
Contract F44620-75-C-0062

ELECTRO-OPTICS LABORATORY
LOCKHEED PALO ALTO RESEARCH LABORATORY
LOCKHEED MISSILES & SPACE COMPANY, INC.
A SUBSIDIARY OF LOCKHEED AIRCRAFT CORPORATION

UNCLASSIFIED

SECURITY CLASSIFICATION OF THIS PAGE (When Data Entered)

REPORT DOCUMENTATION PAGE

READ INSTRUCTIONS BEFORE COMPLETING FORM

1. REPORT NUMBER: AFOSR-TR-76-1100	2. GOVT ACCESSION NO.
3. RECIPIENT'S CATALOG NUMBER	
4. TITLE (and Subtitle): CORKSCREW EFFECT STUDY.	5. TYPE OF REPORT & PERIOD COVERED: Final Report. 2 Feb 1975 – 30 June 1976
6. PERFORMING ORG. REPORT NUMBER: LMSC-D508187	
7. AUTHOR(s): M. W. Munn, R. S. Benson	8. CONTRACT OR GRANT NUMBER(s): F44620-75-C-0062 NEW
9. PERFORMING ORGANIZATION NAME AND ADDRESS: Lockheed Palo Alto Research Laboratory, 3251 Hanover Street, Palo Alto, CA 94304	10. PROGRAM ELEMENT, PROJECT, TASK AREA & WORK UNIT NUMBERS: 61102F, 9767Ø1 NP
11. CONTROLLING OFFICE NAME AND ADDRESS: Air Force Office of Scientific Research (AFSC), Bolling Air Force Base, Bldg. 410, Washington, D.C. 20332	12. REPORT DATE: August 1976
	13. NUMBER OF PAGES: 59
14. MONITORING AGENCY NAME & ADDRESS (if different from Controlling Office): 62p.	15. SECURITY CLASS. (of this report): Unclassified
	15a. DECLASSIFICATION/DOWNGRADING SCHEDULE

16. DISTRIBUTION STATEMENT (of this Report): AF-9767

Approved for public release; distribution unlimited. 9767Ø1

17. DISTRIBUTION STATEMENT (of the abstract entered in Block 20, if different from Report)

18. SUPPLEMENTARY NOTES

TECH OTHER

19. KEY WORDS (Continue on reverse side if necessary and identify by block number)

High energy laser propagation; thermal blooming; non-steady-state; non-coplanar slew

20. ABSTRACT (Continue on reverse side if necessary and identify by block number)

Linearized hydrodynamic equations are solved for the time-dependent density perturbation caused by propagation of a high energy laser beam. The transverse flow of air through the beam (due to any combination of wind, laser platform motion and slew angular velocity) can have any desired time dependence, both in magnitude and direction. At any distance z along the beam the solution gives the variation in refractive index (proportional to the density variation) as a function of position in a plane perpendicular to the optical axis,

(Continued-over)

DD FORM 1 JAN 73 1473 EDITION OF 1 NOV 65 IS OBSOLETE

210118

UNCLASSIFIED

SECURITY CLASSIFICATION OF THIS PAGE (When Data Entered)

Wave optics calculations are made for the propagation of a beam subject to wind plus non-coplanar slew (for the steady-state situation). A scaling law is found for predicting the focal-plane peak irradiance from suitable coplanar calculations.

TABLE OF CONTENTS

Section		Page
1.0	INTRODUCTION	1
2.0	SOLUTION FOR ONE SPATIAL DIMENSION	5
	2.1 Basic Equations	9
	2.2 Linearized Equations	10
	2.3 Inhomogeneous Wave Equation for the Density	12
	2.4 Integral Transformations of the Wave Equation	15
	2.5 Solution for the Density Perturbation	17
	2.6 The Constant Velocity Beam	20
	2.7 The Isobaric Approximation	25
	2.8 Comparison of Constant Velocity and Accelerated Beams	27
	2.9 References	34
3.0	TWO-DIMENSIONAL THERMAL BLOOMING FOR ARBITRARY TRANSVERSE WIND	35
	3.1 Mathematical Solution	36
	3.2 Comparison with the One-Dimensional Solution	39
	3.3 Density Variations within an Accelerated Beam	42
	3.4 References	45
4.0	IRRADIANCE PROFILES FOR NON-COPLANAR SLEW AND WIND	47
	4.1 Scenario Definition	48
	4.2 Scaling Considerations	49

1.0 INTRODUCTION

Key parameters in the assessment of effectiveness of high energy laser systems are the peak intensity and spot size in the focal plane. These two features are strongly influenced by interactions between the laser beam and the atmosphere in the propagation path. The primary interaction of concern here is heating of the atmosphere due to absorption and the hydrodynamics of the heating induced density changes in the air. Specification of parameters such as peak intensity then becomes a problem of specifying in detail the nature of this self-induced atmospheric lens through which the beam must pass.

In addition to molecular absorption, which sets the scale on how much energy is available to cause distortions in the medium, the other critical factor is the rate at which air flows across the beam. The amount of heating experienced by a parcel of air, and hence its distorting power as a lens, is determined by the amount of time it resides within the laser beam. The extent to which the laser beam itself is distorted is then a strong function of the details of the flow field. Important limiting assumptions have been made in theoretical analyses of this effect which is commonly called thermal blooming. These generally include:

- Steady state conditions prevail
- Flow rates are constant (space* and time)
- Time dependence only for zero flow

Actual high energy laser engagements will generally violate one or more of these assumptions. The hydrodynamical formulations which describe the laser -

* To account for slew, the flow velocity is normally allowed to increase linearly with distance along the beam.

atmosphere interactions must, for these engagements, be cast in a form such that the assumptions listed above are not required. The study reported here dealt with these limitations and consists of two distinct segments, namely

- Analytical studies of hydrodynamics
- Wave optics propagation calculations

The hydrodynamical formulation chosen must be general enough to permit description of cases which include

- Non coplanar slew and wind
- Stagnation zones
- Accelerated beams
- Variable winds along the beam

all of which are likely to be encountered in typical engagements. Given hydrodynamical solutions applicable to air flow conditions as above, the effects on laser beam properties (e.g. focal plane irradiance) must be determined by performing wave optics propagation calculations for a beam transmitted through density profiles as determined self consistently for the local laser beam-air interaction.

In Section 2.0, we show the detailed solution to the hydrodynamical equations for one spatial dimension. In this formulation, the wind velocity may vary in magnitude with time and density perturbations in the medium may be tracked from beam turn on to the steady state - if, in fact, the steady state is ever attained in times of interest. The primary advantage of this derivation is its physically intuitive foundation. The various factors which

drive the blooming process separate into components which have clear physical interpretations. In the multi-dimensional theory, given in Section 3.0, this ability to clearly identify specific physical interactions is frequently lost in the details of the mathematics. The formulation, however, permits flow velocities across the beam to be completely arbitrary in magnitude, direction, and time dependence. Computations of density contours and focal plane irradiance profiles, for this more detailed multi-dimensional theory, are shown in Section 4.0.

2.0 SOLUTION FOR ONE SPATIAL DIMENSION

For predicting thermal blooming of a laser beam propagating in the atmosphere, it is usually assumed that the unperturbed airflow through the beam is independent of time. This assumption is not valid for a slewed laser beam in the presence of wind, as well as in the obvious cases of variable wind velocity or slew rate.

Considerable theoretical work has been done on the problem of time-dependent changes in the density of a medium through which a constant-velocity laser beam is propagating. Recently, Ellinwood and Mirels[3] calculated two-dimensional density profiles within a slewed laser beam for both subsonic and supersonic wind transverse to the beam, using linearized hydrodynamic equations. Hayes[6] has addressed the non-linear effects to be expected when the slew rate is near the sound speed, using one-dimensional equations. Fleck et al.[4] have developed an elaborate "four-dimensional" computer code for calculating thermal blooming, based essentially on steady-state equations for the density, but capable of treating supersonic as well as subsonic wind speeds. All these treatments assume both the wind speed and direction to be constant at a given position along the beam.

We here present the general time-dependent solution to the linearized one-dimensional hydrodynamic equations for a beam with an arbitrary, time-dependent intensity profile and which moves with variable velocity. For large-diameter beams and relatively short irradiation times, the effects of

conductivity and convection are expected to be small and have been neglected (cf. Ref. 5). Particular solutions for accelerated, Gaussian CW beams are compared with our analytic solution for a Gaussian beam moving at constant velocity. Greatest differences between the solutions occur for beams which are moving at mach numbers near zero or unity. Density changes within an accelerated beam can be either larger or smaller than for an unaccelerated beam moving at the same speed.

For the purpose of obtaining the density perturbation we assume the unperturbed medium to be at rest while the laser beam moves through it. Of course, this is fully equivalent to the case of wind blowing past a stationary beam, and is a good approximation for a slewed beam as long as nearly sonic slewing velocities do not occur near the beam's point of origin.

For convenience, Table I lists the symbols used in this paper, although the variables are also defined when they are first used in the text.

TABLE I. DEFINITION OF SYMBOLS

Hydrodynamic Variables

ρ	mass density; ρ_o is ambient, unperturbed density
r	density perturbation divided by ρ_o
$R(k,t)$	Fourier transform of $r(x,t)$
$\tilde{R}(k,s)$	Laplace transform of $R(k,t)$
p	fluid pressure
ϵ	specific internal energy
γ	ratio of specific heats
c	speed of sound
v	fluid velocity

Independent Variables

t	time
x	spatial coordinate measured from beam center at t=0
s	parameter appearing in Laplace transform
k	spatial wavenumber appearing in Fourier transform

Properties of the Beam

$x_o(t)$	position of beam center
a	beam radius
ξ	spatial coordinate measured from beam center
V	instantaneous velocity of beam with respect to fluid
M	Mach number of beam, V/c
P	total beam power

TABLE I. (Continued)

$I(x,t)$	beam irradiance
ϕ	normalized irradiance
$F(k,t)$	Fourier transform of ϕ
$\tilde{F}(k,s)$	Laplace transform of F

Heating Rate

α	atmospheric attenuation coefficient
Q	rate of energy deposition per unit volume of fluid
q	normalized (dimensionless) rate of energy deposition

Time Scales

t_H	hydrodynamic time, a/c
Δt_{eq}	time for reaching steady-state perturbation
τ	beam acceleration time-scale

2.1 Basic Equations

The fundamental equations describing the interaction of the laser beam with the atmosphere are (cf. Ref. 7)

$$\frac{d\rho}{dt} + \rho \nabla \cdot \vec{v} = 0 \tag{1}$$

$$\frac{d\vec{v}}{dt} + \frac{1}{\rho} \nabla p = 0 \tag{2}$$

$$\rho \frac{d}{dt} \left[\frac{1}{2} v^2 + \epsilon \right] + \nabla \cdot (p\vec{v}) = Q, \tag{3}$$

which represent conservation of mass, momentum and energy, respectively. The fluid density, velocity, and pressure are denoted by ρ, $\vec{v}$, and p; $Q(\vec{x},t)$ is the heating rate, and is given by

$$Q = \alpha I(\vec{x},t), \tag{4}$$

where α is the atmospheric absorption coefficient and I is the laser irradiance. The specific internal energy of the gas, ϵ, is given by

$$\epsilon = \frac{1}{(\gamma-1)} \frac{p}{\rho}, \tag{5}$$

where γ is the ratio of specific heats. Using the above equations, equation (3) is easily put into the form

$$\frac{dp}{dt} - \gamma \frac{p}{\rho} \frac{d\rho}{dt} = (\gamma - 1) \alpha I \tag{6}$$

2.2 Linearized Equations

The time derivatives appearing in these equations are Lagrangian derivatives, i.e., in operator form

$$\frac{d}{dt} = \frac{\partial}{\partial t} + \vec{v} \cdot \nabla \ . \tag{7}$$

For small-amplitude perturbations of an initially uniform fluid at rest, to first order the $\vec{v} \cdot \nabla$ terms may be reglected and $d/dt \simeq \partial/\partial t$ (Ref. 8). Considering now only fluid flow in one spatial dimension denoted by the coordinate x, the linearized forms of equations (1), (2) and (6) become

$$\frac{\partial \rho}{\partial t} + \rho_o \frac{\partial v}{\partial x} = 0 \tag{8}$$

$$\rho_o \frac{\partial v}{\partial t} + \frac{\partial p}{\partial x} = 0 \tag{9}$$

$$\frac{\partial p}{\partial t} - \frac{c^2}{\gamma - 1} \frac{\partial \rho}{\partial t} = \alpha I, \tag{10}$$

where second and higher order terms have been omitted; denoting the unperturbed pressure and density by p_o and ρ_o respectively, the speed of sound in the undisturbed gas is given by

$$c = (\gamma \ p_o/\rho_o)^{1/2} \ . \tag{11}$$

In equations (8) - (10), and throughout the following development, dependent variables without subscripts denote small perturbations; for example, the total density is given by $\rho_o + \rho$, where $|\rho| \ll \rho_o$.

When the beam moves at constant velocity with respect to the unperturbed air, it is convenient to introduce a new spatial variable,

$$\xi \equiv x - x_o(t), \tag{12}$$

where $x_o(t)$ is the position of beam center at time t. For definiteness, we take the origin of spatial coordinates to be the beam center at t=0 (when the beam is turned on) and assume the beam moves toward positive x. Then, with $x_o = Vt$, the derivatives with respect to t in equations (8) - (10) are transformed as follows*:

$$\frac{\partial}{\partial t} \rightarrow \frac{\partial}{\partial t} - V \frac{\partial}{\partial \xi} . \tag{13}$$

The (ξ,t) coordinates are particularly convenient for describing the perturbation within the beam.

If V is not constant, the transformation (12) is not useful for two reasons. First, the resulting partial differential equations contain terms in which derivatives are multiplied by the non-constant coefficient, V(t). Second, because (ξ,t) is an accelerated reference frame, the quantity dV/dt would appear on the left-hand side of the momentum equation; since it does not possess a (spatial) Fourier transform, it would be necessary to take the gradient of the momentum equation in order to apply this transform. Our procedure is to solve for the density perturbation in (x,t) coordinates, then to use equation (12) to evaluate the solution in the region of interest (i.e., for relatively small values of ξ).

---

* Note that the wind blows with velocity -V with respect to the beam.

2.3 Inhomogeneous Wave Equation for the Density

From equations (8) - (10), it is easy to derive a single equation for the density:

$$\left(\frac{\partial^2}{\partial t^2} - c^2 \frac{\partial^2}{\partial x^2}\right) \frac{\partial \rho}{\partial t} = (\gamma-1) \frac{\partial^2}{\partial x^2} (\alpha I). \tag{14}$$

Integrating with respect to time, we obtain:

$$\left(\frac{\partial^2}{\partial t^2} - c^2 \frac{\partial^2}{\partial x^2}\right) \rho = (\gamma-1) \frac{\partial^2}{\partial x^2} \int_0^t \alpha I(x,t')\, dt', \tag{15}$$

using the conditions

$$\rho = \frac{\partial \rho}{\partial t} = \frac{\partial^2 \rho}{\partial t^2} = 0 \text{ at } t = 0, \quad -\infty < x < \infty \tag{16}$$

(Ref. 10). Equation (15) clearly reveals that the density perturbation is a superposition of waves, with the laser heating acting as driving force.* Physically, energy absorbed from the beam produces local expansion which generates waves traveling outward at the speed of sound. At time t_o after the beam is turned on, $\rho(x,t_o)$ is non-zero over the interval $-ct_o \le x \le ct_o$. However, the solution is not a superposition of simple (adiabatic) sound waves because of the input of energy to the gas within the beam.

---

* Our solution to this equation presumes that $I(x,t)$ is a known function; this is a necessary first step in calculating the actual intensity of a laser beam propagating through perturbed air.

Before solving equation (15), it is convenient to introduce dimensionless variables -- physical quantities are measured in units which are particularly relevant to the problem, and continual repetition of c^2, $(\gamma-1)$, α, etc. is avoided. Introducing the units defined in Table II, equation (15) becomes

$$\left(\frac{\partial^2}{\partial t^2} - \frac{\partial^2}{\partial x^2}\right) r = q \frac{\partial^2}{\partial x^2} \int_o^t \phi(x,t')\, dt', \tag{17}$$

where, for example, $r(x,t)$ denotes the actual density perturbation divided by the ambient, unperturbed density, ρ_o.

TABLE II. DIMENSIONLESS UNITS

QUANTITY	UNIT OF MEASURE	VALUE AT 10 KM ALTITUDE
r, Density Perturbation	ρ_o, Ambient	$\rho_o \sim 4 \times 10^{-4}$ g cm^{-3}
M, Velocity	c, Sound Speed	$c \sim 300$ m sec^{-1}
x, ξ Distance	a, Beam Radius	Assume a = 0.5 m
t, Time	$t_H = a/c$	$t_H \sim 2 \times 10^{-3}$ sec
ϕ, Beam Irradiance	$I_o = P/\pi a^2$	$I_o \simeq 1.27$ P
q, Energy Deposition	$q \equiv \frac{(\gamma-1)\alpha I_o t_H}{\rho_o c^2}$	$q \sim 2 \times 10^{-8}\ \alpha P$
	= Energy absorbed in time t_H ÷ Ambient enthalpy	for α in km^{-1} P in kw

2.4 Integral Transformations of the Wave Equation

To carry out the solution of equation (17), we apply Fourier and Laplace transforms; to define notation, the Fourier transform of a function $g(x,t)$ is given by

$$G(k,t) \equiv \int_{-\infty}^{\infty} e^{-ikx}\, g(x,t)dx, \tag{18}$$

and the Laplace transform of $G(k,t)$ is denoted by

$$\tilde{G}(k,s) \equiv \int_{o}^{\infty} e^{-st}\, G(k,t)dt. \tag{19}$$

Applying these transforms to equation (17) results in

$$[s^2 + k^2]\, \tilde{R}(k,s) = -qk^2\, \tilde{F}(k,s)/s. \tag{20}$$

This equation is valid if the functions r and ϕ (whose transforms are $\tilde{R}$ and $\tilde{F}$, respectively) satisfy certain continuity and boundedness conditions (cf. Ref. 2). To obtain a solution we assume that the boundary conditions [eq. (16)] and the nature of the physical problem prevent the appearance of subtle mathematical pathology.

Formally, the solution for $\rho(x,t)$ is given by the inverse transform of

$$\tilde{R}(k,s) = \frac{-q\tilde{F}(k,s)\, k^2}{s(s^2 + k^2)}, \tag{21}$$

where $\tilde{F}$ is presumed known. For a beam with constant intensity profile and which moves such that its center at time t is located at $x_o(t)$,

$$\phi(x,t) = \phi(x-x_o). \tag{22}$$

Using the translation property of the Fourier transform we have

$$F(k,t) = e^{-ikx_o(t)} \int_{-\infty}^{\infty} e^{-ikx}\, \phi(x)\, dx, \tag{23}$$

where $\phi(x)$ gives the spatial distribution of intensity as a function of distance from beam center. A Gaussian beam, for example, is described by

$$\phi(x) = \exp(-x^2) \tag{24}$$

(recall that distances are measured in units of the beam radius, a). To obtain $\tilde{F}(k,s)$ from equation (23), it is necessary to take the Laplace transform of $\exp[-ikx_o(t)]$.

2.5 Solution for the Density Perturbation

To seek a more fruitful approach, we go back to equation (21), expanding the denominator in partial fractions:

$$\tilde{R}(k,s) = \frac{q\tilde{F}(k,s)}{2} \left\{ \frac{1}{s-ik} + \frac{1}{s+ik} - \frac{2}{s} \right\}. \tag{25}$$

The convolution theorem for the Laplace transform enables us to write the Fourier transform of $r(x,t)$ as a convolution:

$$R(k,t) = q \int_0^t F(k,t') \, G(k,t-t') \, dt', \tag{26}$$

where $G(k,t)$ is the inverse Laplace transform of

$$\tilde{G}(k,s) \equiv \frac{1}{2} \left\{ \frac{1}{s-ik} + \frac{1}{s+ik} - \frac{2}{s} \right\}; \tag{27}$$

explicitly,

$$G(k,t) = \frac{1}{2} \left(e^{ikt} + e^{-ikt} \right) - 1 \tag{28}$$

and

$$R(k,t) = \frac{1}{2} q \int_0^t F(k,t') \left[e^{ik(t-t')} + e^{-ik(t-t')} - 2 \right] dt'. \tag{29}$$

Because of the translation property of Fourier transforms, for any given values of t and t', $F(k,t') \, e^{\pm ik(t-t')}$ is the Fourier transform of $\phi[x \pm (t-t'), t']$. Therefore, taking the inverse Fourier transform of equation (29), we obtain

$$r(x,t) = \frac{1}{2} q \int_0^t \left\{ \phi[x + (t-t'), t'] + \phi[x - (t-t'), t'] \right\} dt' - q \int_0^t \phi(x,t') \, dt', \tag{30}$$

which is the formal solution for the density perturbation.

The meaning of equation (30) becomes clearer if we consider a beam described by equation (22); then

$$\phi[x \pm (t-t'), t'] = \phi[x \pm (t-t') - x_o(t')]. \qquad (31)$$

The expression $x \pm (t-t')$ represents the position at time $t' < t$ of a sonic impulse which will pass the point x at time t; the minus sign corresponds to an impulse moving in the positive x direction (a "forward-facing characteristic") and the plus sign, to a wave moving toward negative x ("backward facing characteristic"). The argument of ϕ in equation (31) is therefore the distance (at time t') between the beam center and the characteristics passing through the point (x,t), and the first two terms on the right-hand side of equation (30) represent the effect at (x,t) due to energy which was absorbed at points on the characteristics during the interval 0 to t. Figure 1 is a space-time diagram which illustrates the geometry involved. The dashed curves on either side of $x_o(t')$ represent the spatial extent of the beam, within which power absorption is greatest. As shown, the point (x,t) has been within the beam for several hydrodynamic times (since $t' \simeq 6.5$) and the resultant absorbed energy contributes an expansion of the air, given by the last term of equation (30). In addition, air with $4 \leq x \leq 6$ has been within the beam at times such that effects of the perturbation can propagate to (x,t). Adding energy to a small volume of air produces local expansion; the "snowplow" effect on neighboring volume elements produces a positive density perturbation outside the originally heated volume. The net perturbation, as given by equation (30) is therefore a superposition of these two effects.

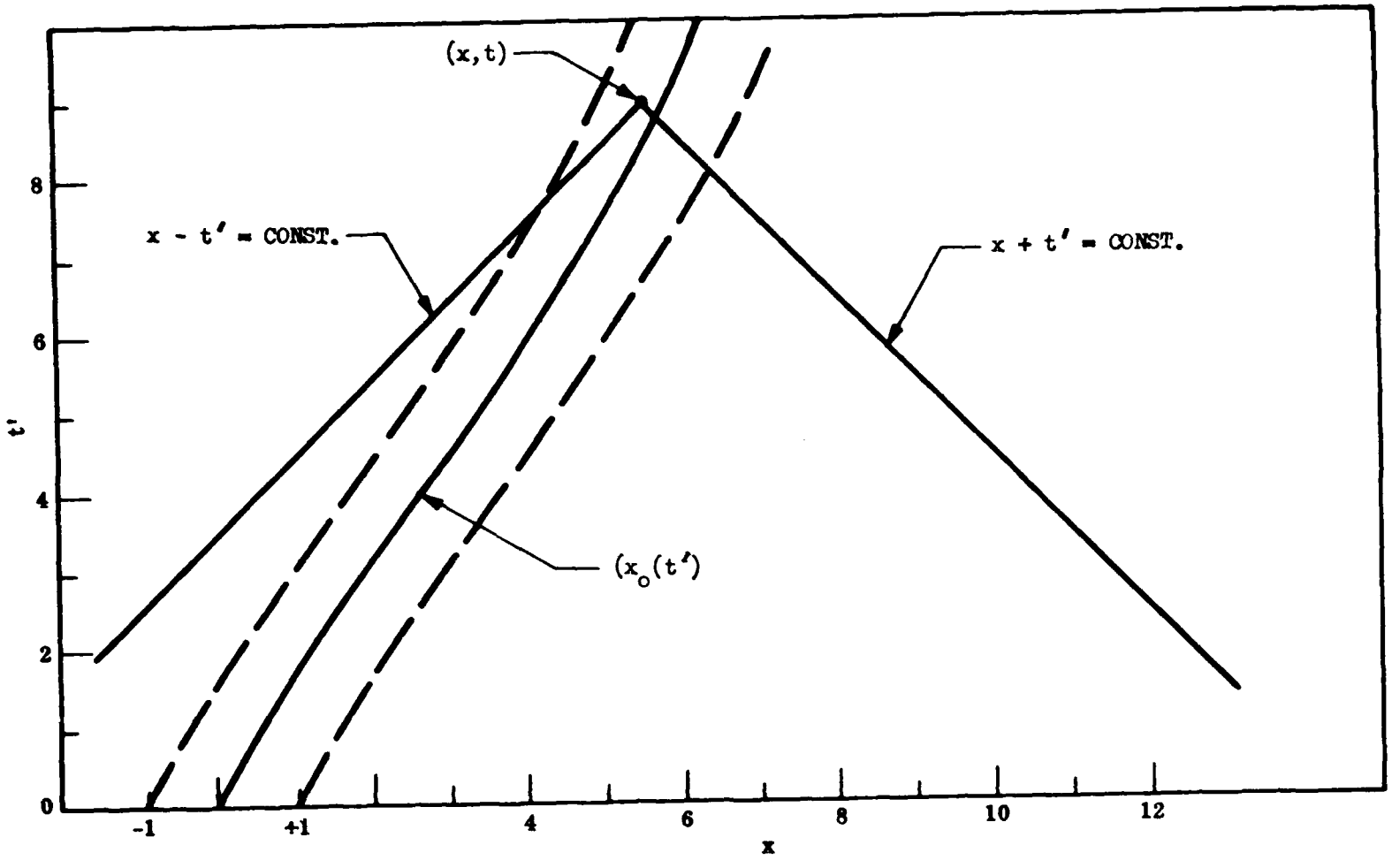

Figure 1. Space-time diagram: $x - t' = \text{CONST.}$, $x + t' = \text{CONST.}$ are characteristics passing through (x,t); $x_o(t')$ is the path of the beam center, while the dashed curves enclose the region of maximum absorbed power.

2.6 The Constant Velocity Beam

As a special case, we can evaluate equation (30) for a beam moving at constant velocity (or, equivalently, a stationary beam and a constant transverse wind). Put

$$x_o(t) = Mt, \tag{32}$$

where M is the mach number for the unperturbed flow. Using equation (31), i.e., assuming the intensity of the beam is constant, the integrals for r(x,t) are of the form

$$\int_0^t \phi\,[x \pm t - (M \pm 1)t']dt'. \tag{33}$$

Defining a variable $y \equiv x \pm t - (M \pm 1)t'$, (33) can be written as

$$-\frac{1}{M \pm 1} \int_{x\pm t}^{x-Mt} \phi(y)dy. \tag{34}$$

For a Gaussian beam (cf. eq. [24]), the integral is

$$\frac{\sqrt{\pi}}{2} \frac{\mathrm{erf}(x\pm t) - \mathrm{erf}(x-Mt)}{M\pm 1} \tag{35}$$

(for properties of the error function, erf(z), see, e.g., Ref. 1). We are primarily interested in the density profile within the beam itself, so introducing the displacement from beam center (ξ is defined in Eq. (12)), the solution becomes

$$r(\xi,t) = \frac{\sqrt{\pi}\,q}{2} \left\{ \frac{1}{2} \frac{\mathrm{erf}[\xi + (M+1)t]}{M+1} + \frac{1}{2} \frac{\mathrm{erf}[\xi + (M-1)t]}{M-1} - \frac{\mathrm{erf}(\xi + Mt)}{M} - \frac{\mathrm{erf}(\xi)}{M(M+1)(M-1)} \right\}. \tag{36}$$

This function is sketched in Figure 2 at a time for which the profile within the beam is near its steady-state shape. The point $\xi = 0$ (at beam center) moves to the right at speed M, leaving behind a low-density region which grows larger with time (it extends to $x = 1$). At time t the perturbed region is confined to $|x| \approx t$, r goes to zero over a distance $\Delta x = 1$ (i.e., the beam radius). Although within the beam r reaches a steady-state after a finite time interval, the true steady-state density is reached as $t \to \infty$; for $M^2 < 1$

$$r(\xi,\infty) = \lim_{t\to\infty} \rho(\xi,t) = \frac{\sqrt{\pi}\, q}{2} \frac{\operatorname{erf}(\xi) - (1-M-M^2)}{M(1-M)(1+M)} . \qquad (37)$$

It is worth pointing out that to obtain the correct steady-state density for the one-dimensional problem, the conditions at infinity cannot be assumed to be unperturbed. From equation (37) the steady-state conditions at spatial infinity are

$$r(\infty, \infty) = \frac{\sqrt{\pi}\, q}{2(1-M)}$$

$$r(-\infty, \infty) = \frac{\sqrt{\pi}\, q}{2(1+M)} . \qquad (38)$$

These non-zero values are due to the fact that in one-dimensional flow without dissipation, the amplitude of a wave does not decrease with distance from the source; for flow in two or three dimensions we would expect to have zero perturbation at infinity.

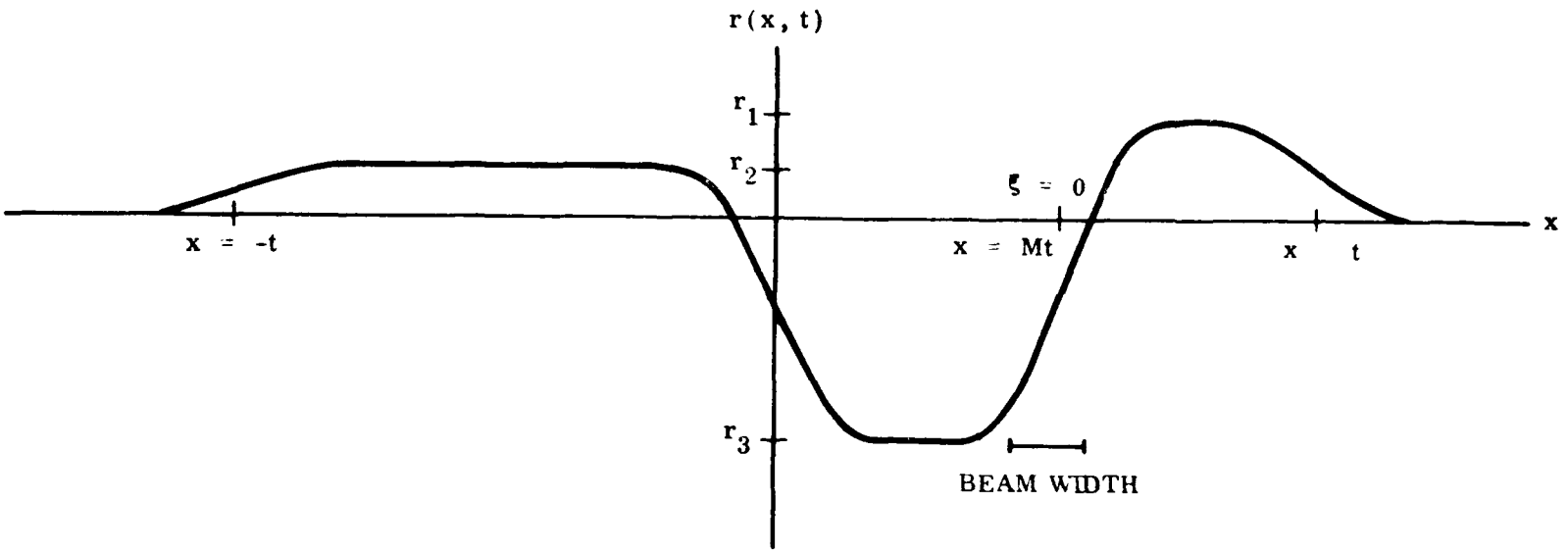

Figure 2. Density perturbation for a constant-velocity beam.

$$r_1 = \frac{q\sqrt{\pi}}{2}\,\frac{1}{1-M}, \quad r_2 = \frac{q\sqrt{\pi}}{2}\,\frac{1}{1+M}, \quad r_3 = -\frac{q\sqrt{\pi}}{2}\,\frac{M+1}{M(M-1)}$$

For supersonic flow $M^2 > 1$, and equation (36) has the steady-state limit

$$r(\xi, \infty) = \frac{\sqrt{\pi}\, q}{2} \frac{1 - \mathrm{erf}(\xi)}{M(M+1)(M-1)} \quad . \tag{39}$$

The air in front of the beam (large ξ) is unperturbed because pressure waves created by the beam propagate more slowly than the beam itself.

Equation (36) also expresses the solution for the special case $M = 1$; proceeding as before, one easily obtains the time-dependent solution

$$r(\xi,t) = \frac{\sqrt{\pi}\, q}{2} \left\{ \frac{t \exp(-\xi^2)}{\sqrt{\pi}} + \frac{1}{2} \frac{1}{4} \left| \mathrm{erf}(\xi+2t) - \mathrm{erf}(\xi+t) \right| + \frac{3}{2} \mathrm{erf}(\xi) \right\} \quad . \tag{40}$$

In this case there is no steady-state. For $t \gg 1$ the first term of equation (40) dominates near beam center; it describes a Gaussian density profile with maximum at beam center. The magnitude of the perturbation grows linearly in time. The present solution remains valid as long as $|r(\xi,t)| \ll 1$, which in turn implies $t \ll 1/10q$. Since expected values of q are much smaller than unity (see Table II), equation (40) describes the sonic case for significant periods of time.

At low wind speeds, the approach to a steady-state within the beam is proportional to the wind transit time, which varies as M^{-1} (cf. Ref. 11). At higher speeds, for $M \sim 1$, sufficient time is required for the forward-moving wave to proceed out of the beam. This wave moves realtive to the

beam at mach number 1-M, so the approach to steady-state is longer as M increases. Quantitatively, the profile given by equation (38) is within 1 percent of the steady-state for $-2 \leq \xi \leq 2$ when $t \geq \Delta t_{eq}$, with

$$\Delta t_{eq} = \max \{4 M^{-1}, 4(1-M)^{-1}\} \quad . \tag{41}$$

As can be seen from Figure 3, the steady-state density change across the beam (from $\xi = -2$ to $\xi = +2$) becomes large as M approaches 0 or 1, although the time required to reach the steady-state (Δt_{eq}) also increases. Time-dependent density profiles given by equation (38) are in complete agreement with Munn's[9] results for the constant velocity beam.

2.7 The Isobaric Approximation

For sufficiently small M, the density perturbation is produced primarily by expansion at nearly constant pressure and the role of outgoing waves is small. The approximate solution is obtained from equation (10) with the pressure perturbation set identically to zero, and is given by the third term on the right-hand side of equation (30). The isobaric solution for a Gaussian beam is

$$r_i = \frac{\sqrt{\pi}\, q}{2} \quad \frac{\mathrm{erf}(\xi) - \mathrm{erf}(\xi + Mt)}{M} \,. \tag{42}$$

The corresponding steady-state density change across the beam is shown in Figure 3 by the dashed curve. The exact solution, equation (36), contains terms which are smaller than those in equation (42) by a factor of approximately M.

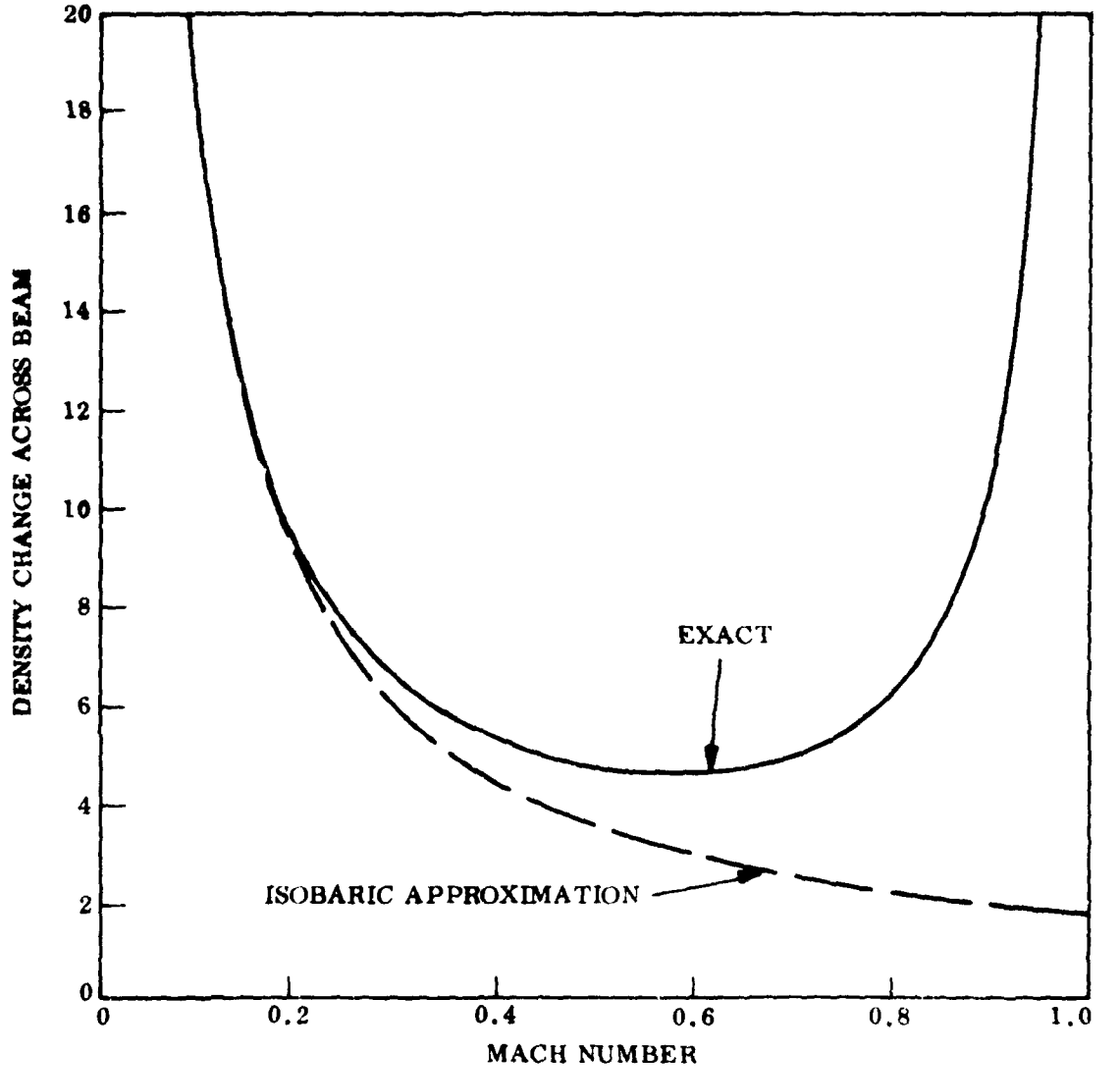

Figure 3. Steady-state density change across a beam moving at constant velocity.

2.8 Comparison of Constant Velocity and Accelerated Beams

In the general case, when the beam moves with arbitrary velocity, the integrals appearing in equation (30) must be numerically evaluated. Note that the beam intensity may also vary arbitrarily, so pulsed beams can be treated as well as CW.

Figure 4 shows the density perturbation for a Gaussian beam moving at $M = 0.1$; when $t = 40$, the profile has essentially achieved a steady-state for $-2 \leq \xi \leq 2$, where the beam is most intense. Figure 5 shows the profile for a beam which initially moves at $M = 0.1$ and is accelerated at the rate $dM/dt = 10^{-3}$ (in dimensionless units); for conditions at 10 km altitude (cf. Table II) this corresponds to an acceleration of 150 m/sec^2. At early times the perturbation does not greatly differ from the constant-velocity case, but by $t = 100$ the departure is obvious. Between $t \simeq 100$ and $t \simeq 700$ the perturbation closely approaches the steady-state profile corresponding to the instantaneous velocity. The later development is shown in Figure 6. As M exceeds 0.8, there develops a density maximum near $\xi = 1$ and, especially for $\xi > 0$, the profile departs more and more from the corresponding steady-state in the sense of having smaller perturbation. As a measure of the perturbation at each instant, we use the differenceiin density from maximum to minimum within $-2 \leq \xi \leq 2$. The solid curve in Figure 7 represents the magnitude of the steady-state perturbation for constant-velocity beams as a function of mach number (from Figure 3). The points connected by a dashed curve represent the profiles shown in Figures 5 and 6; across the top of Figure 7 is the time scale for the accelerated beam. When the beam is turned on at $t = 0$, $M = 0.1$ and the density perturbation is zero. At this speed, a steady-state would be

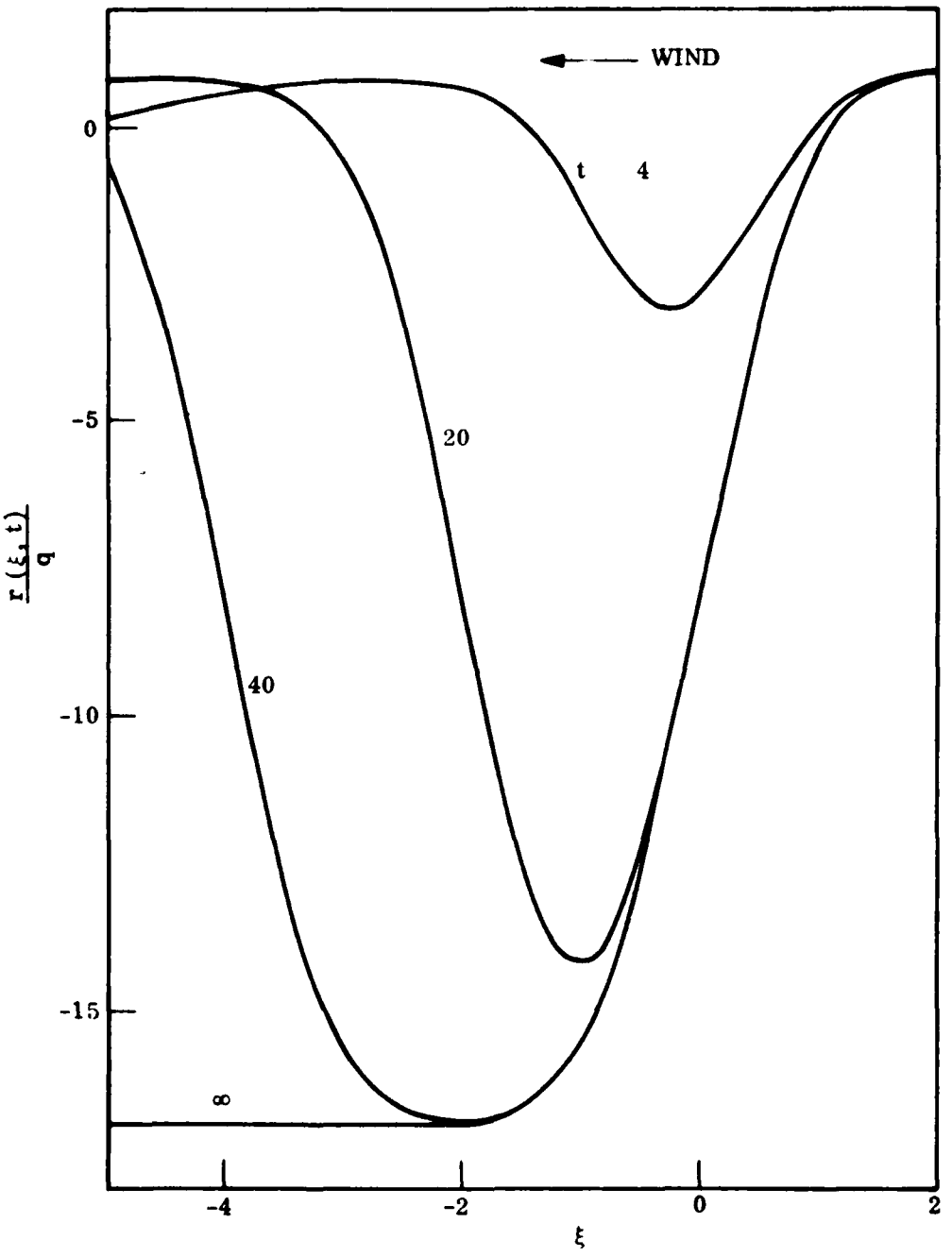

Figure 4. Time-dependent density within a constant-velocity beam moving at M = 6.1.

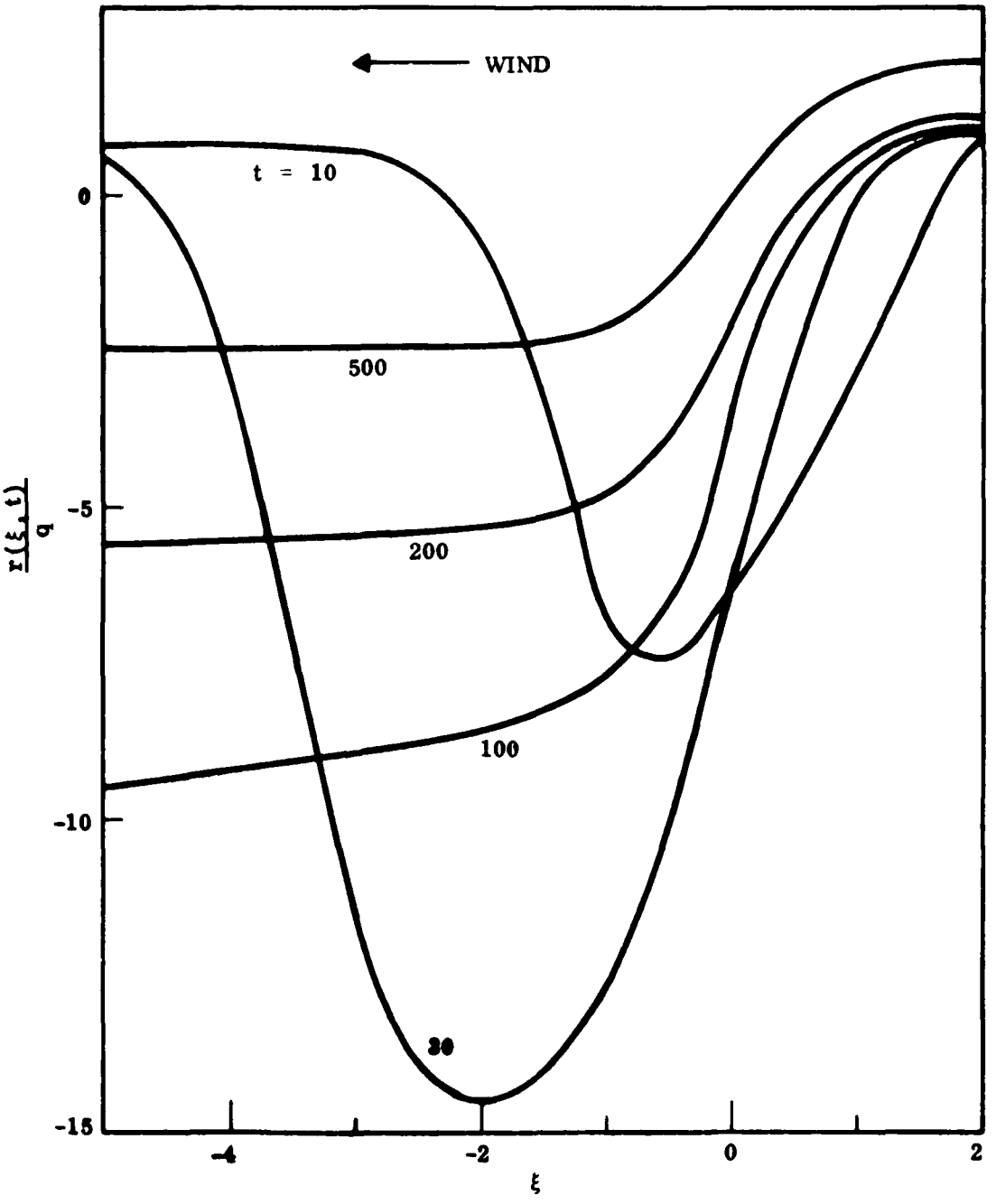

Figure 5. Time-dependent density profiles for an accelerated beam; initially M = 0.1, dM/dt = 0.001. For t ≥ 500, see Fig. 6.

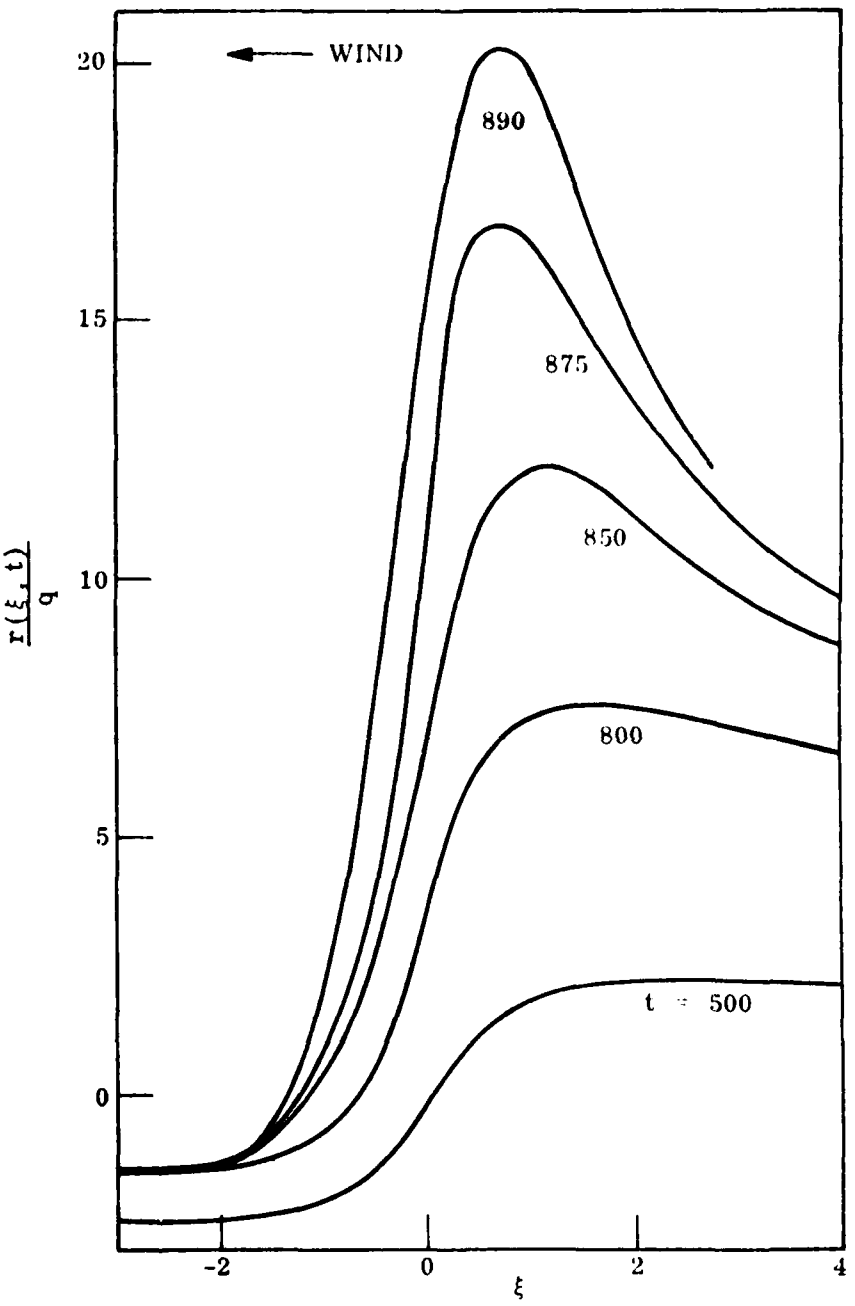

Figure 6. Density profiles for t = 500; same beam as for Figure 5.

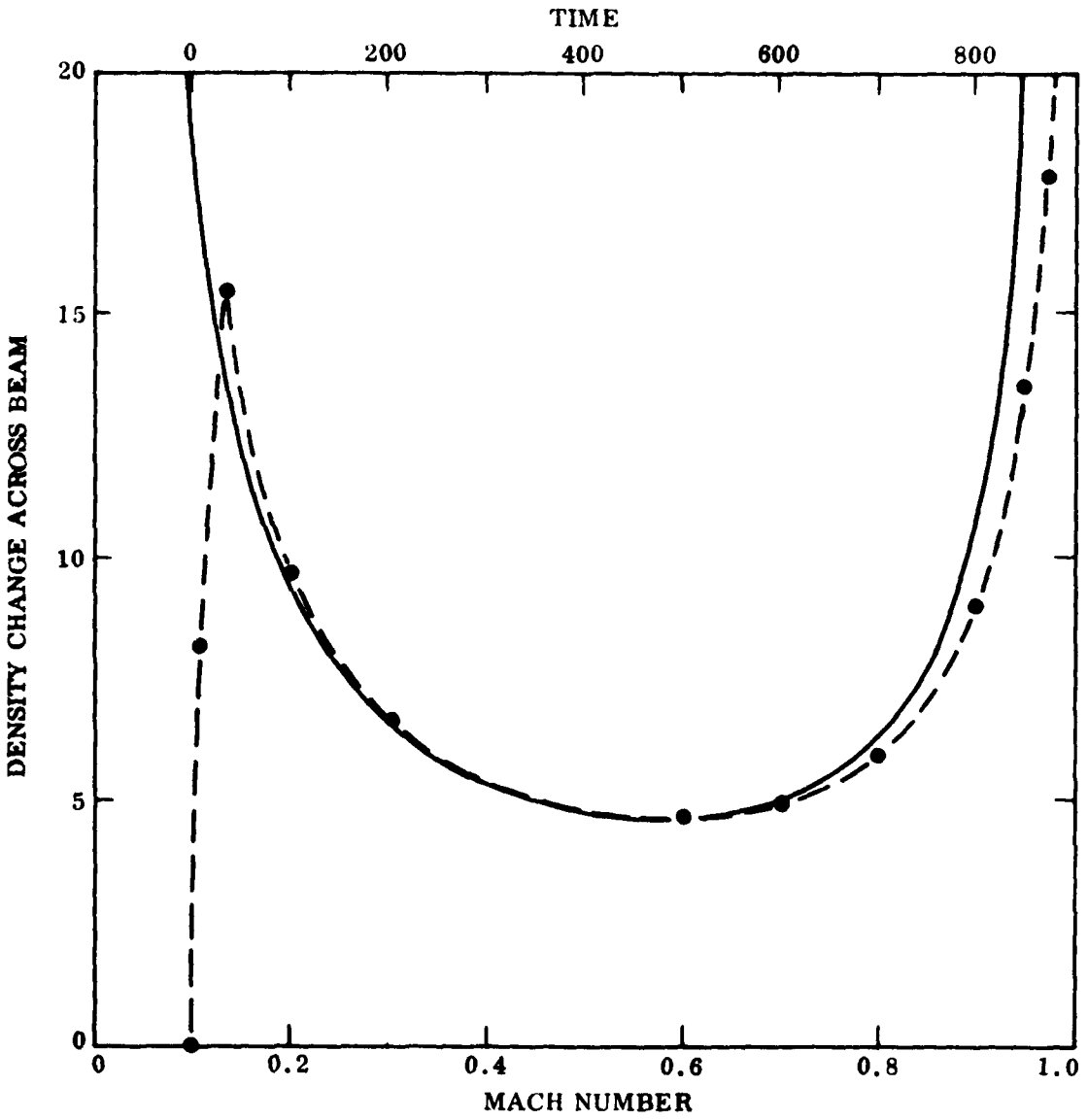

Figure 7. Density change across accelerated beam (points and dashed curve) compared with steady-state conditions for constant velocity beams (solid curve).

reached when $t \simeq 40$, but by that time the beam's mach number has increased to 0.14. The new speed implies a shorter equilibration time and a smaller steady-state perturbation; together with the finite equilibration time, this produces a slightly larger perturbation than would be the case for the instantaneous steady-state. As the beam moves faster, the equilibration time decreases and the perturbation is nearly equal to the corresponding steady-state. Later, when $M \simeq 0.1$, the equilibration time [illegible] and the magnitude of the perturbation lags behind the steady-state.

The perturbation for a decelerated beam is shown in Figure 8. Initially, $M = 0.1$; with $dM/dt = -10^{-3}$, the beam is stationary at $t = 100$ and moves back toward its initial position at later times. When $t \leq 100$, the amplitude of the perturbation is less than the steady-state value, but after $t = 100$, the perturbation considerably exceeds the steady-state value. At $t = 150$, with $M = -0.05$, the steady-state density change across the beam would be approximately $\Delta r \simeq 34q$, while the actual Δr is nearly three times as large.

Defining a time-scale for acceleration by

$$\tau = |M/A|, \tag{43}$$

where $A = dM/dt$ (in dimensionless units), it is possible to estimate those velocities and accelerations for which the density profile will differ significantly from the constant-velocity solution. When τ is smaller than $\Delta\tau_{eq}$, the beam velocity changes more quickly than the density approaches steady-state. Using equation (41), this condition becomes

$$|A| > \min\{M^2/4, (1-M)^2/4\}, \tag{44}$$

from which we see that small accelerations have the greatest effect for $M \simeq 0$ or $M \simeq 1$.

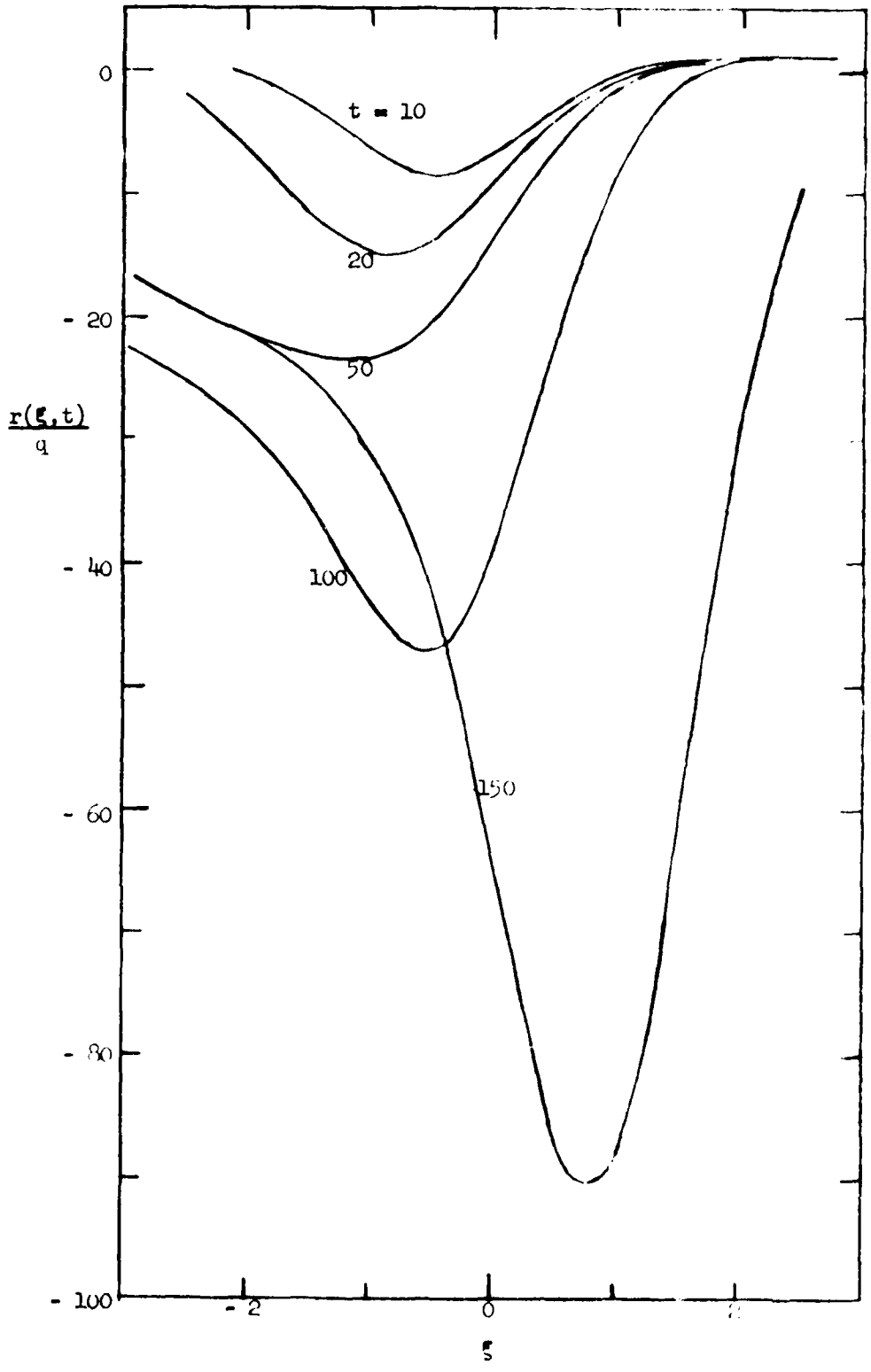

Figure 8. Time-dependent densities within a beam initially moving at M = 0.1, for dM/dt = - 0.001.

2.0 References

1. Abramowitz, M. and I.A. Stegun, eds., Handbook of Mathematical Functions, U.S. Dept. of Commerce, NBS 55, June 1964, Chapter 7.
2. Churchill, R.V.; Operational Mathematics (McGraw-Hill, New York, third ed. 1972).
3. Ellinwood, J.W. and H. Mirels; Appl. Opt. 14, 2238 (1975).
4. Fleck, Jr., J.A., J.R. Morris and M.J. Feit; "Time-Dependent Propagation of High Energy Laser Beams Through the Atmosphere," Lawrence Livermore Laboratory, UCRL-51826, June 2, 1975.
5. Hayes, J.N., Appl. Opt. 11, 455 (1972).
6. Hayes, J.N., Appl. Opt. 13, 2072 (1974).
7. Landau, L.D. and E.M. Lifshitz; Fluid Mechanics (Addison-Wesley, Reading, Mass., 1959).
8. von Mises, R.; Mathematical Theory of Compressible Fluid Flow (Academic Press, New York, 1958), p. 34.
9. Munn, M.W.; "Dependence of Thermal Blooming Induced Density Changes in Gas on Time and Transverse Flow Velocity," Lockheed Palo Alto Research Laboratory, LMSC D403870, July 1974.
10. Ulrich, P.B. and J. Wallace; J. Opt. Soc. Am. 63, 8 (1973).
11. Wallace, J. and M. Camac; J. Opt. Soc. Am. 60, 1587 (1970).

3.0 TWO-DIMENSIONAL THERMAL BLOOMING FOR ARBITRARY TRANSVERSE WIND

It has proven convenient to part from traditional formulations of the laser heating hydrodynamics which assume a simple relationship between Eulerian (beam centered) and Lagrangian (parcel of air centered) coordinate systems. The treatment given here does not assume the transverse flow to be constant in magnitude or direction.[1,2]

In Eulerian coordinates, at a fixed distance z along the beam the wind flowing in the x,y plane (perpendicular to the z-axis) is assumed to be a known function of time:

$$\vec{w}(z,t) = \hat{x}\, w_x(z,t) + \hat{y}\, w_y(z,t) \tag{1}$$

and in general $\vec{w}$ is composed of components due to natural wind, motion of the laser platform, and non-zero slewing of the beam. The Lagrangian formulation consists of expressing the equations of hydrodynamics in the coordinate frame which is at rest in the unperturbed air. In this frame the beam moves with average velocity

$$\vec{v}_b(z,t) = -\vec{w}(z,t) \tag{2}$$

In the discussion below, note that all equations are written in physical variables; dimensionless variables are not introduced.

5.1 Mathematical Solution

In Lagrangian coordinates, in which the unperturbed medium is at rest, small amplitude variations in pressure, density and velocity (denoted by p, ρ and $\vec{v}$, respectively) satisfy the linearized equations:

$$\frac{\partial \rho}{\partial t} + \rho_o \nabla \cdot \vec{v} = 0 \tag{3}$$

$$\rho_o \frac{\partial \vec{v}}{\partial t} + \nabla p = 0 \tag{4}$$

$$\frac{\partial p}{\partial t} - \gamma \frac{p_o}{\rho_o} \frac{\partial \rho}{\partial t} = (\gamma - 1)\, \alpha\, I(\vec{r}, t) \quad . \tag{5}$$

The ambient pressure and density are p_o and ρ_o, γ is the ratio of specific heats and α is the atmospheric absorption coefficient. The beam irradiance I includes time dependence which is due to motion of the beam relative to the unperturbed medium.

Integrating equation (5) with respect to time gives

$$\frac{\rho(\vec{r}, t)}{\rho_o} = \frac{p(\vec{r}, t)}{\gamma p_o} - \frac{(\gamma - 1)\,\alpha}{\gamma p_o} \int_o^t I(\vec{r}, t_o)\, dt_o \quad . \tag{6}$$

On the right-hand side, the first term represents an acoustic (adiabatic) disturbance, while the second term is an isobaric expansion which dominates when the beam moves slowly. The pressure variation p can itself be expressed as an integral of the irradiance multiplied by an appropriate Green's function whereupon substitution into equation (6) gives the solution for ρ in terms of known functions.

Into equation (4) we introduce the vector potential $\psi(\vec{r}, t)$, which is related to the velocity by

$$v = -\nabla\psi \tag{7}$$

It is then easily shown that

$$\frac{p}{\gamma p_o} = \frac{1}{c^2}\frac{\partial\psi}{\partial t} \quad , \tag{8}$$

where $c = (\gamma p_o/\rho_o)^{1/2}$ is the sound speed. As follows from equations (3), (4) and (7), ψ satisfies an inhomogeneous wave equation with source term $(\gamma - 1)\,\alpha I/\rho_o c^2$, and it can be written in terms of a Green's function $G(\vec{r}_o, t_o\,;\,\vec{r}, t)$ which gives the contribution at (r,t) due to energy deposited at $(\vec{r}_o, t_o)$. The time derivative of ψ is then

$$\frac{\partial\psi}{\partial t} = \frac{(\gamma - 1)\,\alpha}{\rho_o c^2}\int_o^t dt_o \int d^3 r_o\; I(\vec{r}_o, t_o)\frac{\partial G}{\partial t} \quad . \tag{9}$$

Morse and Feshbach[3] give the appropriate Green's function for the two-dimensional problem: i.e., for spatial variations in the (x, y) plane normal to the beam and neglecting slow variations along the beam (parallel to the z axis). The spatial integral in equation (9) then reduces to a surface integral which can be expressed in polar coordinates (R, θ) centered at the point (x, y):

$$\begin{aligned} R &\equiv (x - x_o)^2 + (y - y_o)^2 \\ \theta &\equiv \arctan\left[(y - y_o)/(x - x_o)\right] \quad . \end{aligned} \tag{10}$$

The result can be put into the form

$$\frac{\partial\psi}{\partial t} = \frac{(\gamma - 1)\,\alpha}{2\pi\,\rho_o c^2}\int_o^t dt_o \int_o^{2\pi} d\theta\; F(\theta, t_o\,;\,x, y, t) \quad , \tag{11}$$

where[4]

$$F(\theta, t_o ; x, y, t) = I(R_{max}, \theta, t_o) - (t - t_o) \int_o^{R_{max}} R\, dR \frac{I(R, \theta, t_o) - I(R_{max}, \theta, t_o)}{\left|(t - t_o)^2 - R^2/c^2\right|^{3/2}} \tag{12}$$

and $R_{max} = c(t - t_o)$. By choosing the coordinates (x, y) to lie within the beam at time t, the solution is evaluated only at points of interest for calculating thermal blooming.

3.2 Comparison with the One-Dimensional Solution

The Green's function formalism for expressing laser induced density changes makes it somewhat difficult to develop an intuitive understanding of the underlying physics. In order to deomonstrate use of the formalism, and to establish contact with a known and relatively easily solved case, we consider the one-dimensional, constant velocity case discussed in Section 2. For this case equations (6) and (9) become, with $Q = \alpha I$,

$$\rho(x, t) = -\frac{\gamma - 1}{c^2} \int_0^t dt' \left\{ Q(x, t') - \frac{1}{c^2} \int dx' \, Q(x', t) \, \frac{\partial G_1}{\partial t} \right\} \quad (13)$$

and the Green's function, given by Morse and Feshbach, is

$$G_1 = \frac{c}{2} U\left[(t - t') - \frac{1}{c} |x - x'|\right] \quad . \quad (14)$$

the step function $U(z)$ is related to the Dirac delta function: $U'(z) = \delta(z)$. Differentiating G_1 with respect to t gives

$$\frac{\partial G_1}{\partial t} = \frac{c}{2} \left\{ \delta\left(\frac{1}{c}[x - x'] + [t - t']\right) + \delta\left(\frac{1}{c}[x - x'] - [t - t']\right) \right\} \quad . \quad (15)$$

the integral over x' is easily performed, and

$$\rho(x, t) = -\frac{\gamma - 1}{c^2} \int_0^t dt' \left\{ Q(x, t') - \frac{1}{2} \, Q(x + c[t - t'], t') + Q(x - c[t - t'], t') \right\} \quad (16)$$

If the beam intensity is independent of time (in its own rest frame) then Q is a function only of the distance from beam center, i.e.

$$Q(x \pm c[t - t'], t') = Q(x \pm c[t - t'] - x_b[t']) \quad (17)$$

where $x_b(t)$ is the position of beam center at time t. For the special case of <u>constant transverse wind</u> we may put

$$x_b(t) = vt \quad . \tag{18}$$

Note that the wind moves at speed $w = -v$ with respect to the beam and the integrals appearing in equation (16) are of the form

$$\int_0^t dt' \, Q(x \pm c[t - t'] - vt') \tag{19}$$

which can be simplified by the substitution

$$y = x \pm c[t - t'] = x \pm ct - (v \pm c)t' \quad . \tag{20}$$

Then (19) becomes

$$-\frac{1}{v \pm c} \int_{x \pm ct}^{x-vt} Q(y)\, dy \tag{21}$$

To express this result in coordinates which move with the beam, make the transformation

$$\xi = x - vt \tag{22}$$

ξ is the distance from beam center. Equation (21) then becomes

$$-\frac{1}{v \pm c} \int_{\xi + (v \pm c)t}^{\xi} Q(y)\, dy \tag{23}$$

Written out explicitly in terms of the wind speed w, equation (16) now becomes

$$\rho(\xi,t) = \frac{\gamma - 1}{c^2} \left\{ \frac{1}{w} \int_{\xi - wt}^{\xi} Q(y)dy - \frac{1}{2} \left[\frac{1}{c+w} \int_{\xi-(c+w)t}^{\xi} Q(y)dy - \frac{1}{c-w} \int_{\xi-(c-w)t}^{\xi} Q(y)dy \right] \right\} \tag{24}$$

when $|w| \ll c$ the 2nd and 3rd terms are negligible with respect to the 1st term and we have

$$\rho(\xi,t) \simeq \frac{(\gamma - 1)\,\alpha}{c^2\, w} \int_{\xi - wt}^{\xi} I(y)\, dy \quad , \tag{25}$$

which is the familiar form of the solution for the isobaric approximation.[5]

3.3 Density Variations within an Accelerated Beam

Using the equations developed in Section 3.1 we have calculated the thermal blooming density perturbation for an infinite Gaussian irradiance profile. To illustrate the effects of propagation in the presence of stagnation zones, as in Section 2.8, we chose the time-dependence of the beam motion to be

$$v = v_o - at \tag{26}$$

with initial velocity $v_o = 0.1$ c and constant acceleration $a = 10^{-3}\ c^2/\omega \sim 10^2\ \omega^{-1}$ m/sec^2, where ω is the beam radius (in meters). The flow velocity relative to the beam is $w = -v$; at a time Δt after beam turn-on, the flow velocity is momentarily zero, where

$$\Delta t = 0.3\ \omega \text{ sec} \quad . \tag{27}$$

Figure 1 shows density contours for $t \leq 1.5\ \Delta t$. During this interval the density never reaches a steady state, nor can the profiles be approximated by suitably chosen steady state curves.

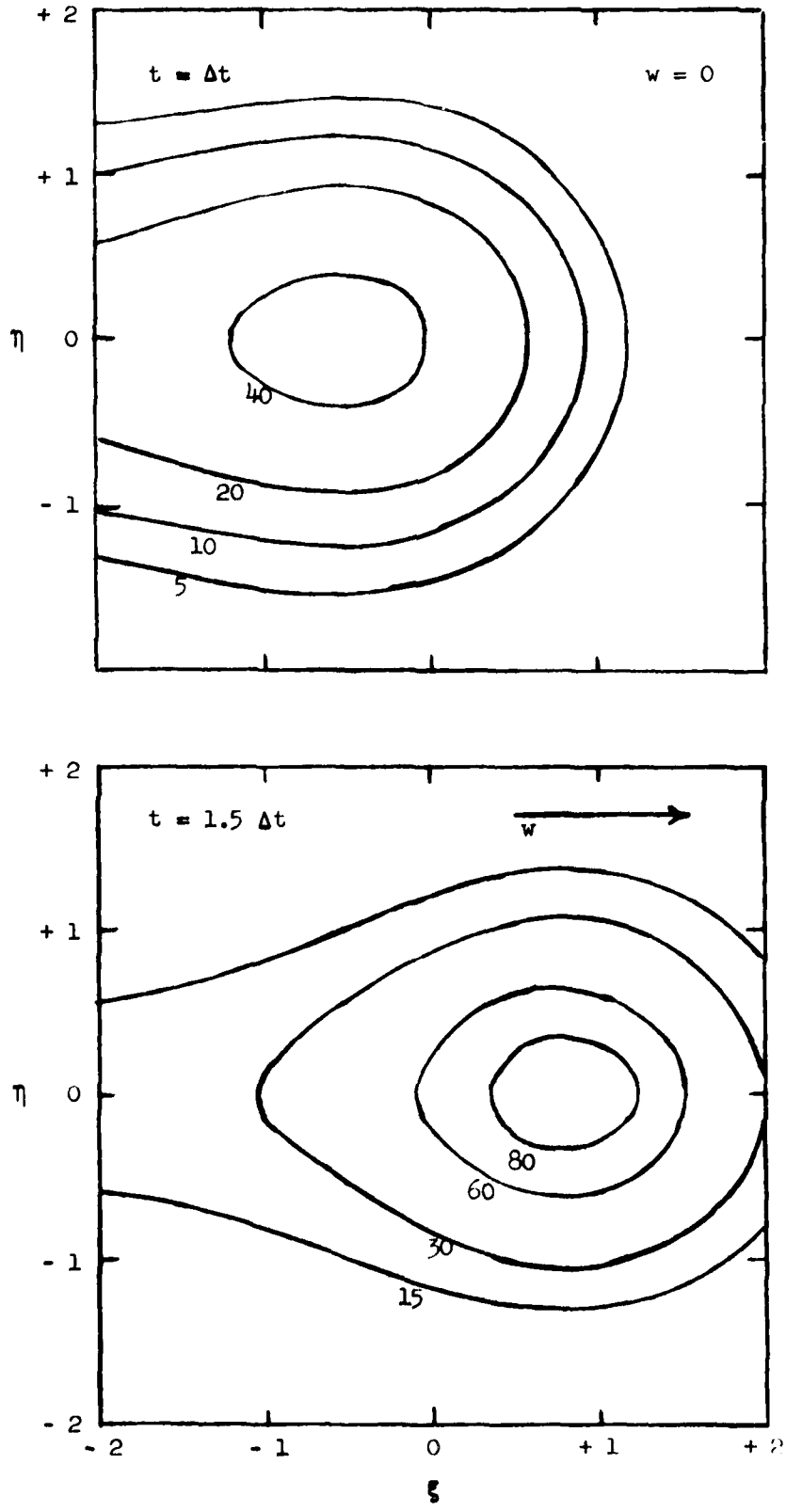

Figure 1 continued

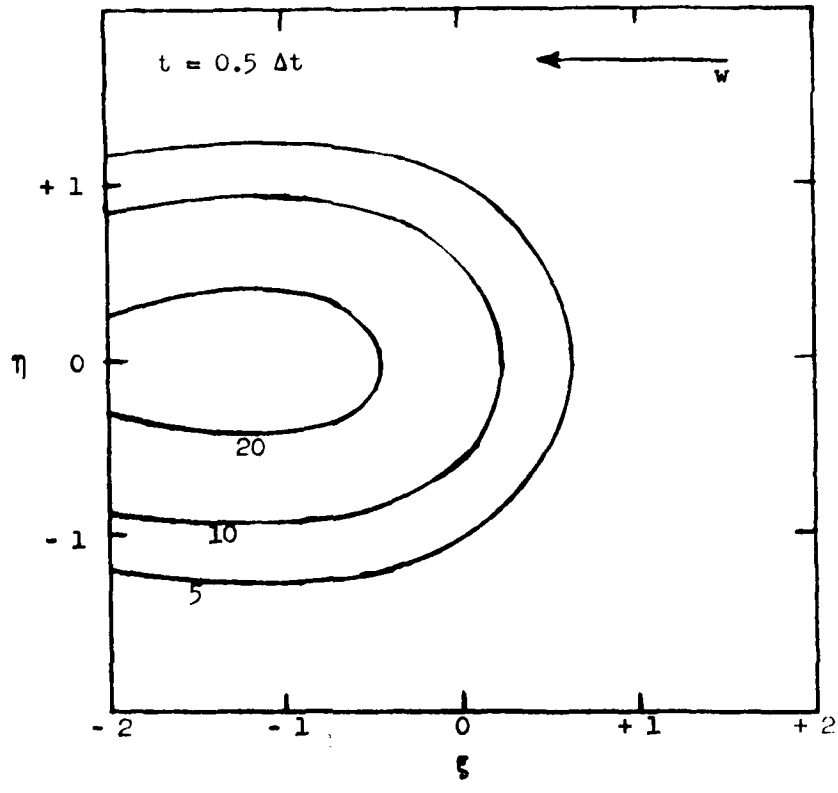

Figure 1. **Density Contours in an Accelerated Beam.** At each time t are shown curves of constant $|\Delta\rho/\rho_o|$ measured in units of $(\gamma-1)\alpha R\omega/\rho_o c^2$. The spatial coordinates (ξ,η) are co-moving with the beam; distances are measured in beam radii, ω. The flow velocity has the same magnitude at t = 0.5 Δt and t = 1.5 Δt, but the density profiles are significantly different both in shape and magnitude.

3.4 References

1. Ellinwood, J. W. and Mirels, H., Appl. Opt. 14, 2238 (1975)

2. Wallace, J. and Pasciak, J., Appl. Opt. 15, 218 (976)

3. Morse, P. M. and Feshback, H., Methods of Theoretical Physics, 893 (N.Y.: McGraw-Hill Book Co. 1953)

4. For careful mathematical treatment of the spatial integral involved here, see Hadamard, J., Lectures on Cauchy's Problem, 117-141 (N.Y., Dover Publications 1952)

5. Hogge, C. B., "Propagation of High-Energy Laser Beams in the Atmosphere," Air Force Weapons Laboratory, Kirtland Air Force Base, New Mexico, AFWL-TR-74-74 (June 1974)

4.0 IRRADIANCE PROFILES FOR NON-COPLANAR SLEW AND WIND

To predict the irradiance within a laser beam propagating through the atmosphere requires a wave optics computer code which includes an evaluation of the laser-induced hydrodynamics which was discussed in earlier sections. Dr. C. B. Hogge of the Air Force Weapons Laboratory in Albuquerque kindly made available to us his wave optics code, which we modified to carry out the computations discussed below.

As a first step toward implementing the mathematical solution derived in Section 3, we replaced the hydrodynamics section of Dr. Hogge's code with coding which calculates two-dimensional density perturbation for arbitrary magnitude and direction of the transverse flow velocity, assuming steady-state conditions obtain. Further generalization of the coding to deal with the fully time-dependent problem is now relatively straightforward. But before making the second step, we made some test calculations which in themselves yielded useful results.

A number of runs were made with the modified propagation code for cases in which the natural wind (perhaps due to laser platform motion) is not coplanar with the non-zero slew velocity. From the results we have found that a simple scaling is possible to predict the peak intensity in the focal plane (under certain conditions) from coplanar data.

4.1 Scenario Definition

Propagation runs were performed for the following set of conditions:

- Co-altitude device and target
- Platform induced flow in the horizontal plane
- Slew plane oriented at arbitrary angles (0° to 180°)* with respect to the horizontal.

A number of different

- Power levels
- Beam sizes
- Kinetic cooling conditions
- Slew rates

were considered. In particular slew rates were adjusted so that the 180° orientation included a case which would have had a stagnation zone, although no calculation was performed for this case.

* At 0° slew and wind velocities are additive and at 180° they subtract; at intermediate angles the vector sum has a non-zero component perpendicular to the horizontal. (This component is a linear function of distance along the beam.)

4.2 Scaling Considerations

A particular subset of the code runs were found amenable to scaling for determining peak intensity levels. The conditions appropriate for this are

- Moderate to little kinetic cooling
- Steady state
- Slew angle less than 90°.

Define in the usual way

$$I_{REL} = I(PEAK, BLOOMED)/I(PEAK, VACUUM, ATTENUATED) \quad (1)$$

where I is the intensity. Also define an effective transverse flow velocity as

$$V_{EFF} = \int_{o}^{R} |\vec{v}(z)| dz/R \quad (2)$$

where

$$\vec{v}(z) = \vec{v}_{\omega} + \vec{\Omega} z \quad (3)$$

and R is range to target.

Here v_{ω} is the natural wind and/or platform motion induced flow and Ω is the slew rate. The vector notation formally signifies that v_{ω} and Ω are not necessarily coplanar.

All calculations shown are for a beam focused on a target 5 km from the transmitter and an absorption coefficient of 0.1 km^{-1}; the platform

velocity is v_ω = 67.0 m/sec (150 mph). As examples of the computational results, Figures 1-3 show the focal-plane irradiance contours for θ = 0, 90° and 120°, respectively. The maximum irradiance occurs at the point marked by the cross; the contours are for the 90%, 50% and 10% irradiance, normalized to the maximum. The slew rate is 0.0268 rad/sec, and the direction of the resultant slew velocity component is shown in each figure. This angular velocity was chosen to give a slew velocity equal in magnitude to v_ω at the half-way point along the beam. Figures 4 and 5 show the magnitude of the flow velocity and its orientation with respect to v_ω as functions of distance along the beam. Figure 4, for θ = 90°, is qualitatively representative of $\theta \leq 90°$ in the sense that the transverse flow velocity is a monotonically increasing function of distance from the transmitter. In contrast, Figure 5 shows how the flow velocity for $\theta > 90°$ (120° in this case) has a minimum between the transmitter and target. The effective velocity (V_{eff}) is defined by equation (2), and is the average along the beam of the magnitude of the flow velocity.

The centroid of the focal spot is displaced from the optic axis of the transmitter (the aim point in the focal plane). This is shown in Figure 6. Increasing θ moves the beam farther from the aim point and away from the horizontal axis.

Figure 7 shows I_{rel} as a function of V_{eff}; each point represents a calculation using a modification of Dr. Hogge's wave optics code. The infinite Gaussian has a spot size of 0.25 m; the slew angular velocity is $\Omega_1 = 2.682 \times 10^{-2}$ rad/sec. From left to right, the points represent

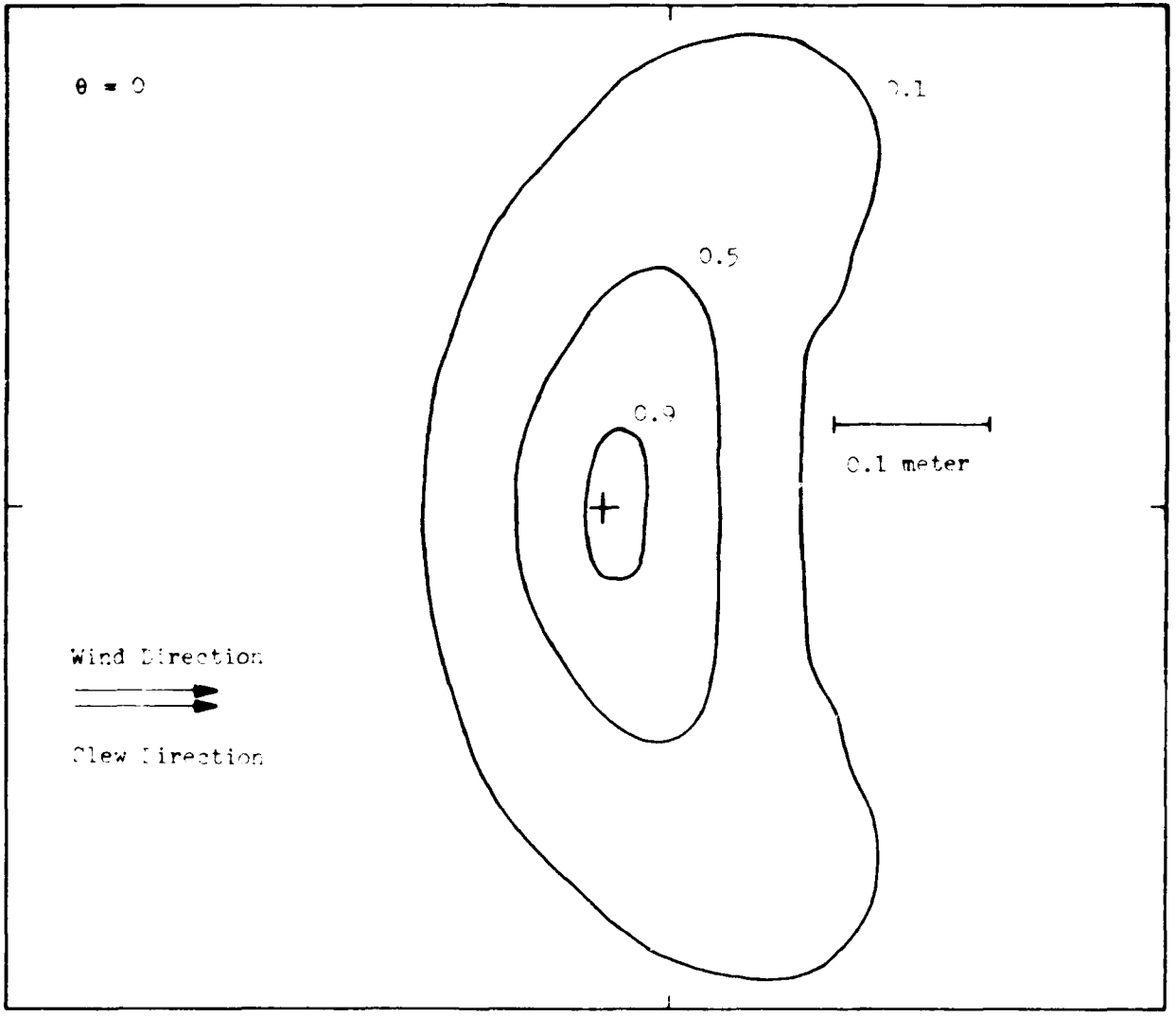

Figure 1. Irradiance contours in the focal plane for coplanar wind and slew (θ = 0).

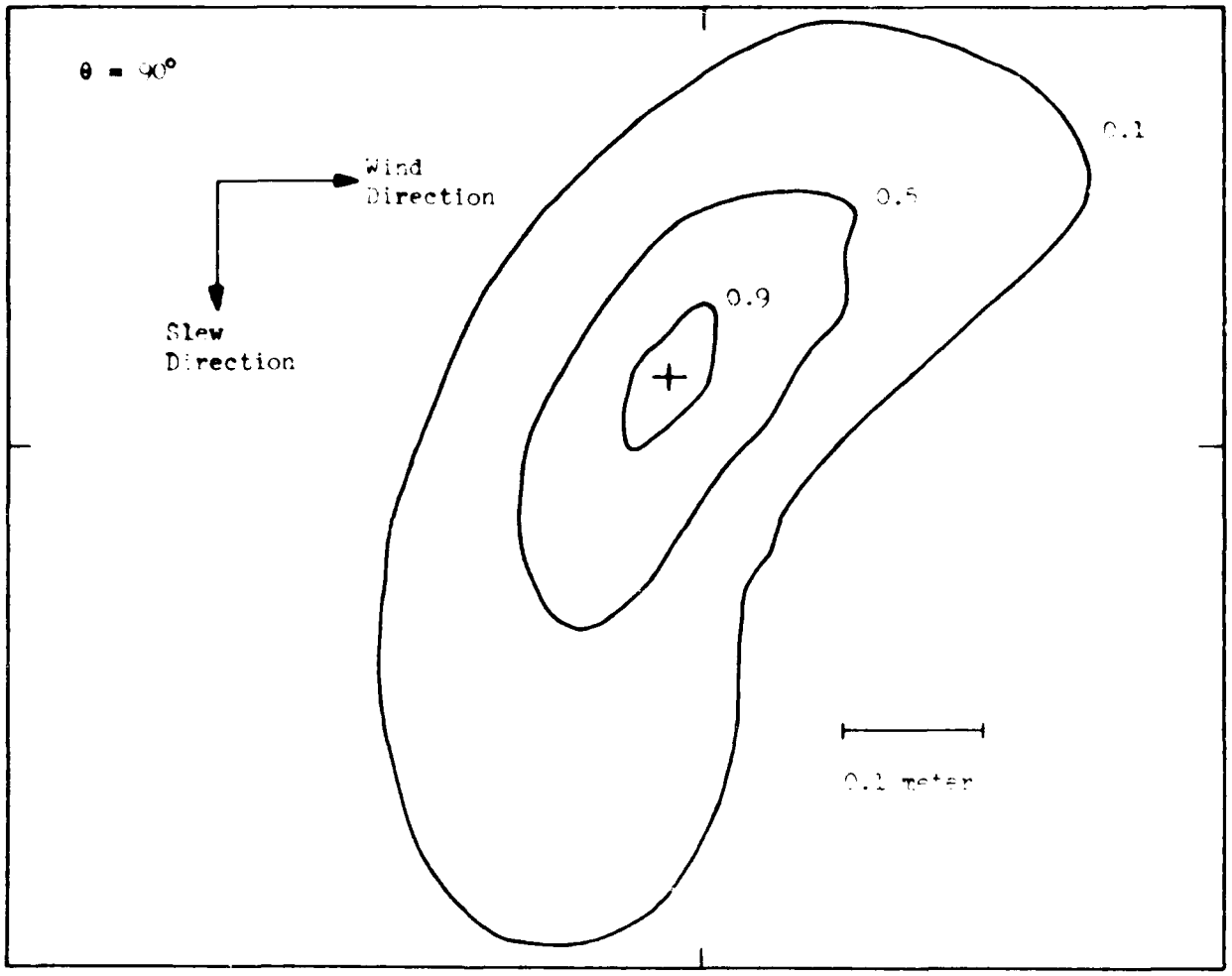

Figure 3. Focal plane irradiance contours. Wind and slew have same magnitudes as in Fig. 1, but here θ = 90°.

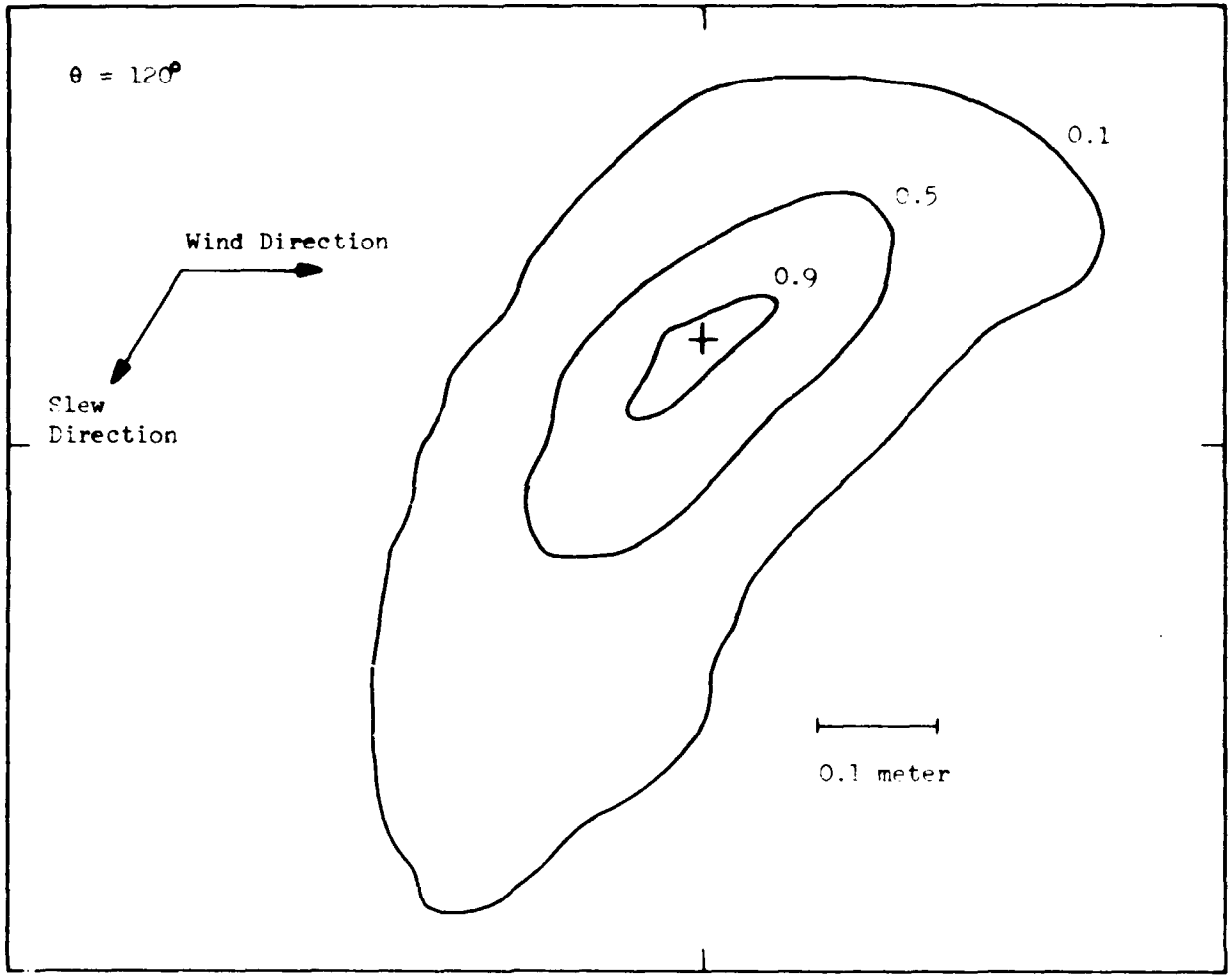

Figure 3. Focal plane irradiance contours for non-coplanar wind and slew ($\theta = 120°$).

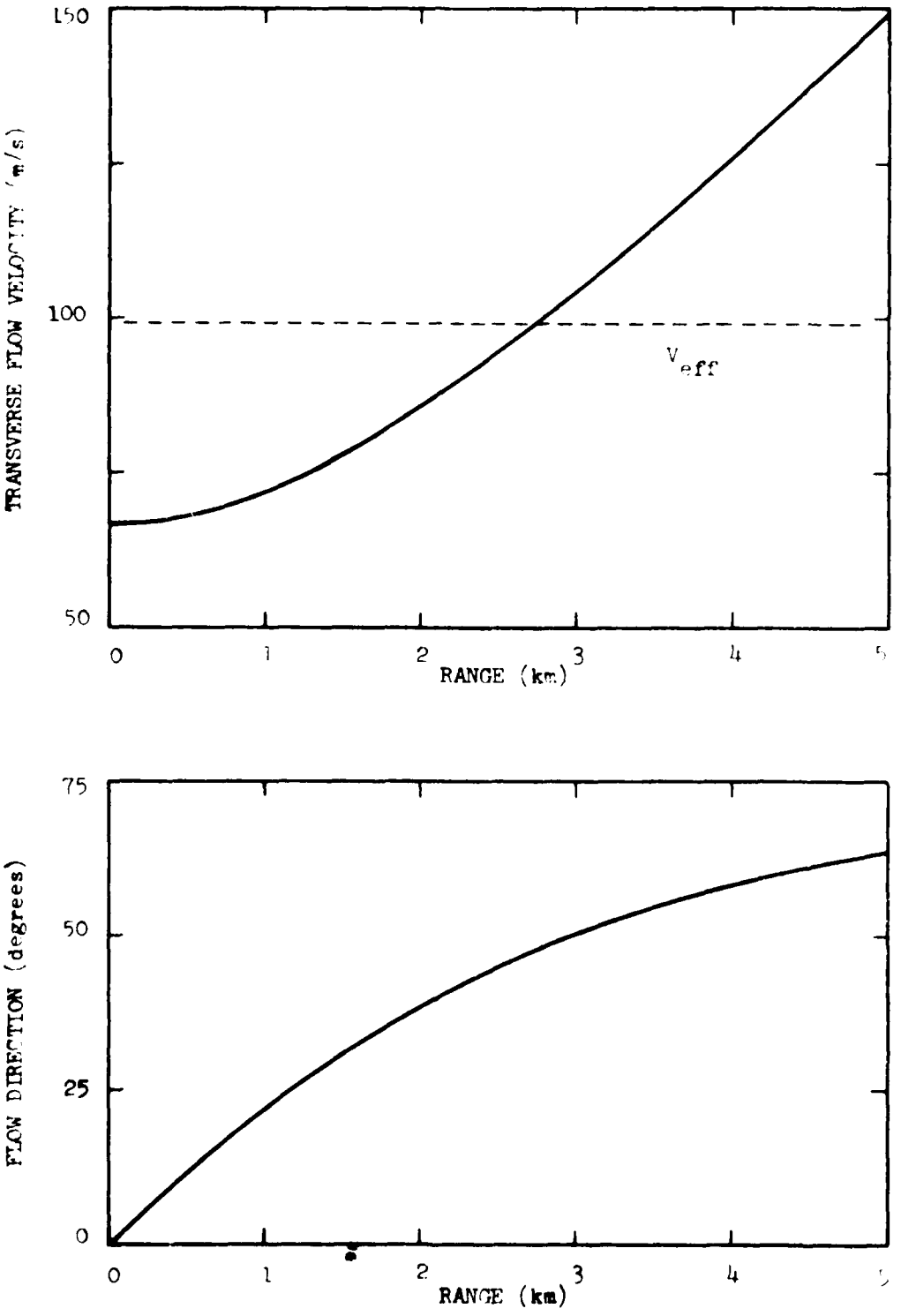

Figure 4. Magnitude and direction (measured from horizontal) of the flow velocity as functions of distance along the beam, for $\theta = 90^\circ$.

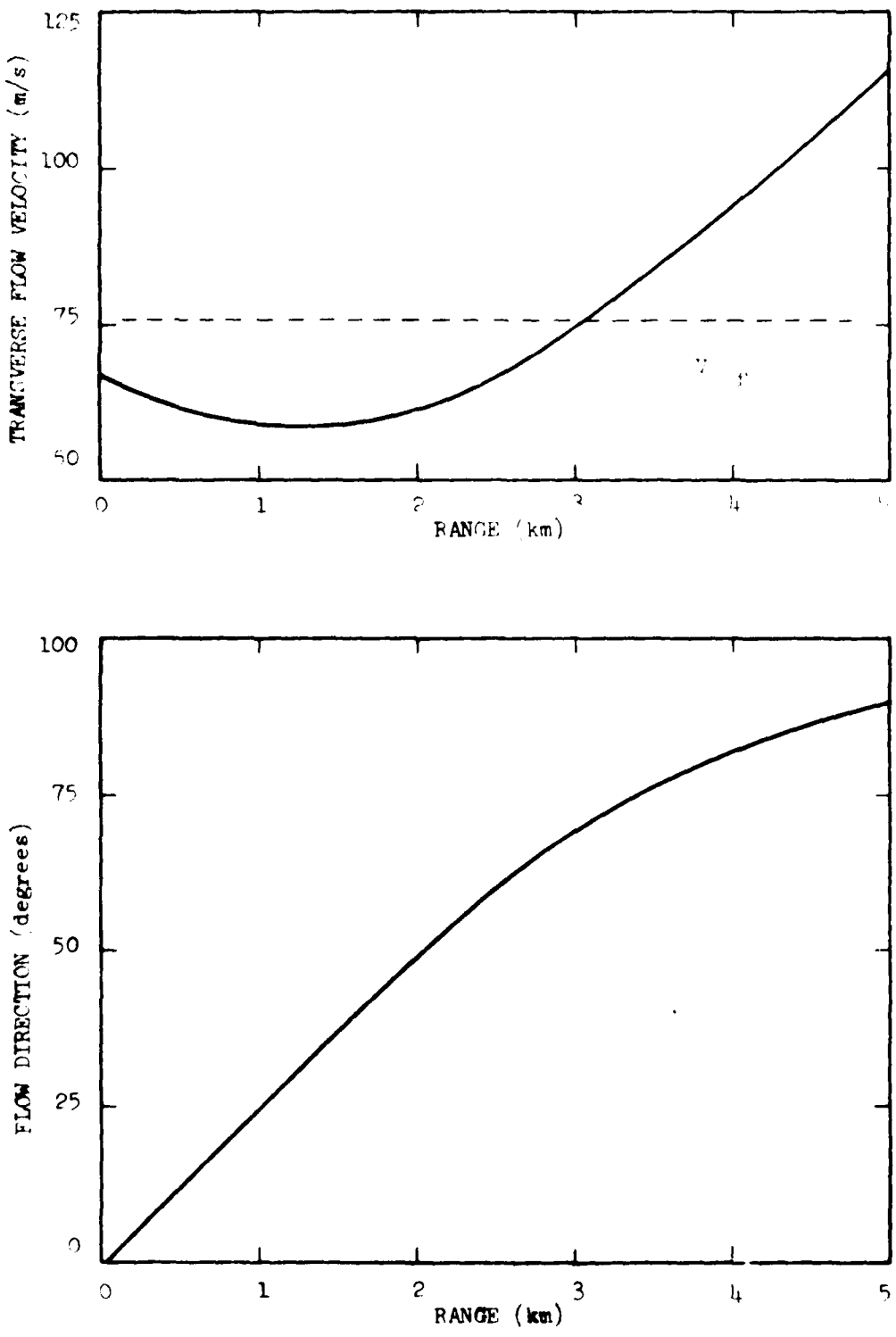

Figure 5. Magnitude and direction (measured from horizontal) of the flow velocity as functions of distance along the beam, for $\theta = 120^{\circ}$.

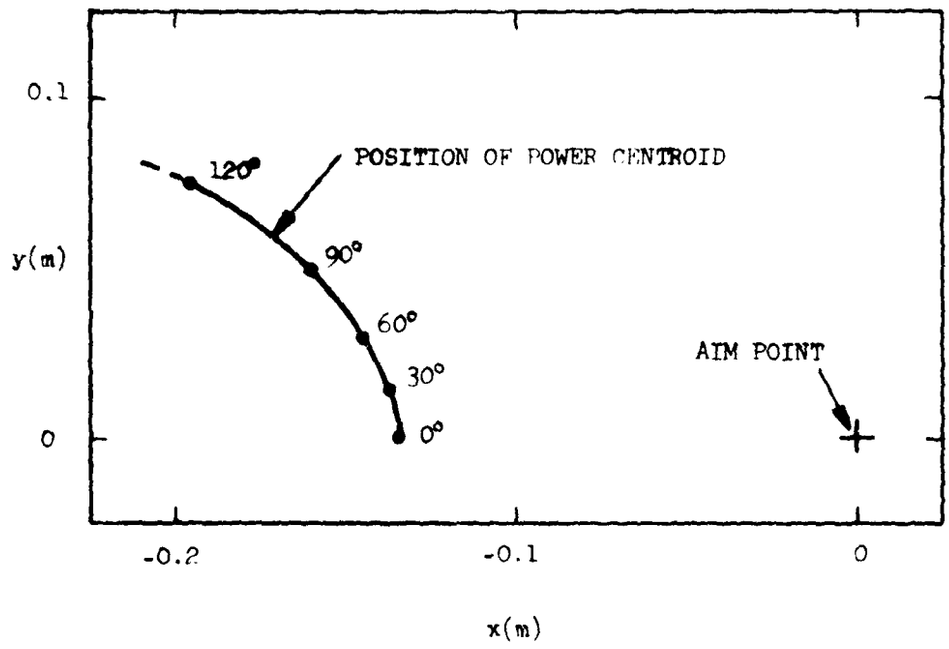

Figure 6. Position in the focal plane of the intensity centroid as a function of angle between slew and wind velocities.

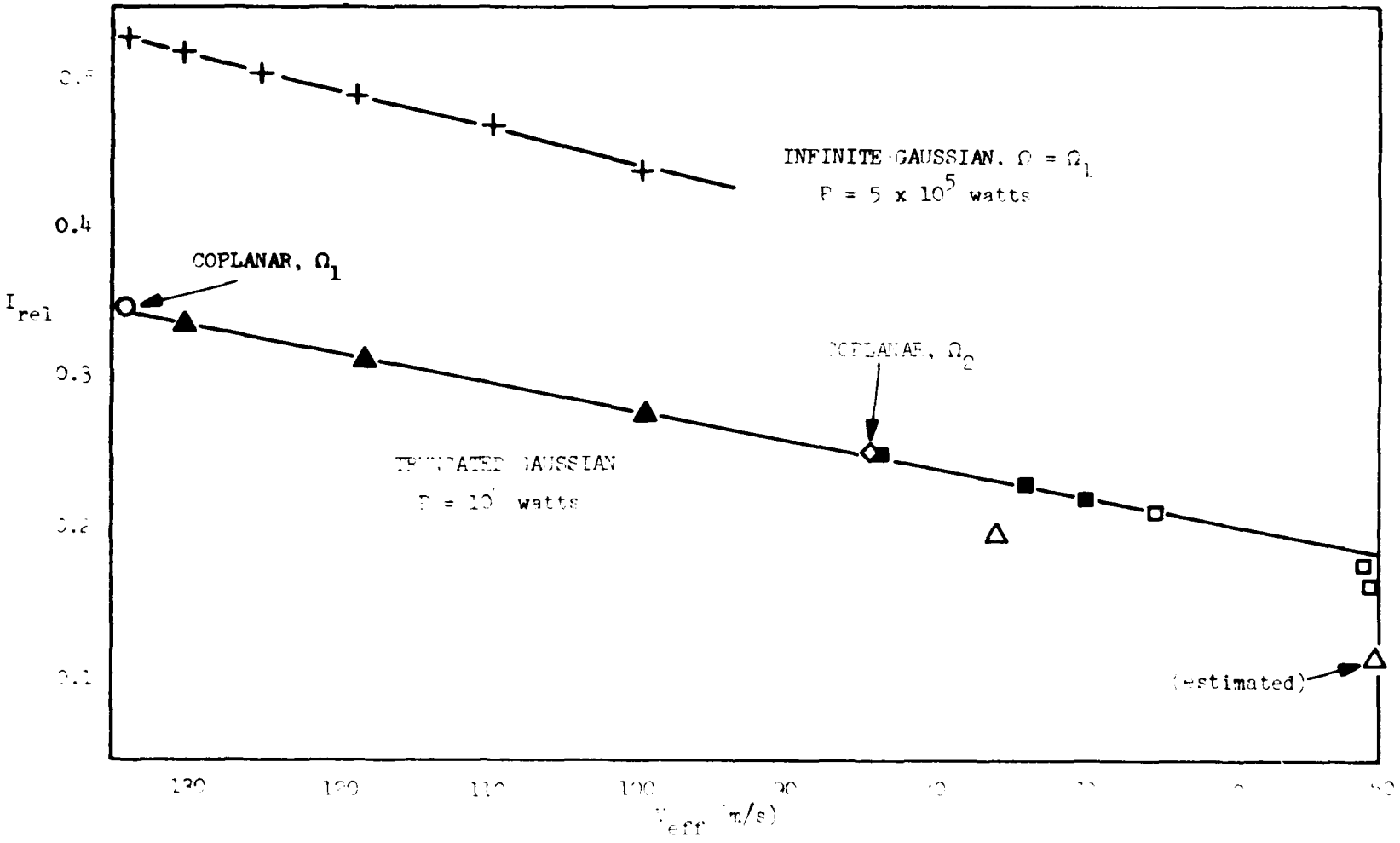

Figure 7. Linear relation between I_{rel} and V_{eff} for non coplanar wind and slew. Filled symbols represent cases with $\theta < 90°$.

$\theta = 15^\circ$, 30°, 45°, 60° and 90°. The truncated Gaussian has a spot size of 0.1768 m; calculations were done for Ω_1 and for $\Omega_2 = 0.5\ \Omega_1$. The coplanar cases are indicated in the figure. The triangular symbols represent non coplanar cases with $\Omega = \Omega_1$, while those for $\Omega = \Omega_2$ are shown as square symbols. The open symbols denote cases with $\theta > 90^\circ$, while filled symbols are for $\theta \leq 90^\circ$. As long as θ is not greater than 90°, there is a striking <u>linear</u> relation between I_{rel} and V_{eff}. This linear dependence resembles the usual scaling laws for coplanar wind and slew; what is demonstrated here is a linear scaling of I_{rel} when the wind and slew are not in the same plane, and the validity of the scaling up to $\theta = 90^\circ$.

With the quantities defined at the beginning of the section, non coplanar peak intensities may be obtained as follows:

a) For a given v_ω, calculate I_{rel} in the standard way for two <u>coplanar</u> cases, (v_ω, Ω_2) with $\Omega_1 \neq \Omega_2 \neq 0$.

b) Using these two values of I_{rel} and the two corresponding values of V_{eff}, derive the straight line $I_{rel} = A\ V_{eff} + B$.

c) For a non coplanar case, calculate V_{eff} for $\vec{v}(z) = \vec{v}_\omega + \vec{\Omega} z$ using Equation (2), then find I_{rel} from the equation derived in Part (b) above.

There is a caveat attached to this which must be strictly observed, namely

a) Magnitude of $\vec{v}(z)$ <u>must</u> be monotone increasing (i.e., θ must be no greater than 90°).

More complicated scalings exist for other cases in the presence of strong kinetic cooling or non monotone increasing velocity magnitudes. Scaling for

these cases requires more parameters. We also note that no conclusions should be drawn regarding beam shape and size as compared to the coplanar case since non symmetrical distortions do occur and the relationship between peak and average intensity changes.